CZECH TECHNICAL UNIVERSITY IN PRAGUE

Faculty of Nuclear Sciences and Physical Engineering

Department of Physics

Bachelor thesis

Detector Control System for the ALICE Experiment

Miroslav Šimko

Supervisor: Doc. RNDr. Vojtěch Petráček CSc.

Prague, 2011

ČESKÉ VYSOKÉ UČENÍ TECHNICKÉ
V PRAZE
Fakulta Jaderná a Fyzikálně Inženýrská
Katedra Fyziky

Bakalářská práce

Řídící systém detektoru ALICE

Miroslav Šimko

Vedoucí práce: Doc. RNDr. Vojtěch Petráček CSc.

Praha, 2011

ČESKÉ VYSOKÉ UČENÍ TECHNICKÉ V PRAZE
FAKULTA JADERNÁ A FYZIKÁLNĚ INŽENÝRSKÁ
PRAHA 1 - STARÉ MĚSTO, BŘEHOVÁ 7 - PSČ 115 19

Katedra: fyziky *Akademický rok:* 2010/11

ZADÁNÍ BAKALÁŘSKÉ PRÁCE

Posluchač: Miroslav Šimko

Obor: Jaderné inženýrství

Zaměření: Experimentální jaderná fyzika

Název práce: Řídící systém detektoru ALICE

Název práce: (anglicky) Detector control system for the ALICE experiment

Osnova:

Student se podrobně seznámí se strukturou a činností řídícího systému (DCS) experimentu ALICE, zejména pak s řídícím systémem křemíkových driftových detektorů. Student provede podrobnou dokumentaci činnosti a ovládání systému a seznámí se s programováním jeho komponent, zejména pak kontrolerů využívajících programovatelná logická pole FPGA a řídícího programu PVSSII. Student bude pracovat na ladění softwarových částí systému. Student se tak připraví na činnosti související s řízením experimentu ALICE, na kterých se bude rovněž podílet.

Doporučená literatura:

1. ALICE Technical Proposal, CERN/LHCC/95-71
2. ALICE DCS Technical Design Report, CERN/LHCC/2001-021

Jméno a pracoviště vedoucího bakalářské práce:

Doc. RNDr. Vojtěch Petráček, CSc., FJFI ČVUT

Do bakalářské práce se vkládá zadání a dále na stranu předcházející obsahu abstrakt a klíčová slova. Součástí zadání bakalářské práce je její uložení na webové stránky katedry fyziky a zaslání abstraktu a klíčových slov ve formátu WORD na e-mailovou adresu katedry fyziky: kf@fjfi.cvut.cz

Datum zadání bakalářské práce: 12.10.2010

Termín odevzdání bakalářské práce: 08.07.2011

.... *Vedoucí katedry*

.... *Děkan*

V Praze dne 12.10.2010

Prohlášení:

Prohlašuji, že jsem svou bakalářskou práci vypracoval samostatně a použil jsem pouze podklady (literaturu, software, atd.) uvedené v přiloženém seznamu.

Nemám závažný důvod proti užití tohoto školního díla ve smyslu § 60 Zákona č. 121/2000 Sb., o právu autorském, o právech souvisejících s právem autorským a o změně některých zákonů (autorský zákon).

V Praze dne 8.7.2011 Miroslav Šimko

Title:
Detector Control System for the ALICE Experiment

Author: Miroslav Šimko

Specialization: Experimental nuclear physics

Sort of project: Bachelor thesis

Supervisor: Doc. RNDr. Vojtěch Petráček CSc.
Consultant: Ing. Radek Šmakal

Abstract: The main subject of this bachelor thesis is the detector control system (DCS) for the ALICE experiment with special emphasis on the silicon drift detector (SDD) of the inner tracking system (ITS). The ALICE detector with all its sub-detectors and its detector control system are described. Moreover, this work contains more detailed informations about the ITS and its SDD layers. In addition, the DCS system for the SDD is described. A commercial SCADA system PVSS was chosen as the core software for the DCS. One of my tasks in this project was to learn the basics of programming in the PVSS program.

Key words: control system, DCS, ALICE, ITS, SDD, PVSS

Název práce:
Řídící systém detektoru ALICE

Autor: Miroslav Šimko

Abstrakt: Tato bakalářská práce se zabývá řídícími systémy na detektoru ALICE se zaměřením na křemíkové driftové detektory (SDD) vnitřního dráhového systému ITS. Práce popisuje experiment ALICE se všemi subdetektory a jeho řídícím systémem. Poskytuje také podrobnější popis vnitřního dráhového systému a hlavně jeho driftových detektorů. Dále je také popsán řídící systém driftových detektorů. Jako softwarové jádro řídícího systému byl zvolen program PVSS, v němž bylo mým úkolem se naučit vytvářet aplikace.

Klíčová slova: řídící systém, DCS, ALICE, ITS, SDD, PVSS

Acknowledgement

I would like to thank Doc. RNDr. Vojtìch Petráèek CSc. for his professional assistance and remarks, and especially Ing. Radek Šmakal for his help with the PVSSII program, remarks concerning the professional side and grammar of this work, and general help with this bachelor thesis. I would also like to thank Ing. Jiří Král for his help with the PVSSII and information about the ALICE DCS, and Jarka Hrtánková and Jakub Škoda for their grammar check.

Contents

Chapter 1

Introduction

The main task of this bachelor thesis was to get familiar with the Detector Control System (DCS) for the ALICE experiment with emphasis to the Silicon Drift Detector (SDD) of the Inner Tracking System (ITS). Therefore, most of this work consists of description of the ALICE detector, ITS and SDD and their detector control system.

The core software of the DCS is a commercial SCADA (Supervisory Controls and Data Acquisition) system: PVSSII. As I am planning to contribute to the development of the software for the DCS in the future, it was necessary to learn the basics of the PVSSII program. Some of my applications in PVSS will be described, as well as the PVSSII itself.

This thesis consists of three basic parts:

The introductory part (chapters 2 and 3) describes the ALICE detector and its involved sub-detectors, and the detector control system for ALICE. Moreover, the main parameters of the ALICE sub-detectors are written down and explained. Also, the reader will get familiar with the main characteristics of the ALICE DCS.

The second part (chapters 4 and 5) deals with the inner tracking system, and especially the silicon drift detectors which are described in more detail, along with their detector control system. In this part, the six layers of the ITS are described: two layers of the silicon pixel detectors, mainly the two of the silicon drift detectors and two of the silicon strip detectors. Moreover, the structure of the detector control system for the SDD is explained.

The third part (chapter 6) shows some informations about the PVSSII and my applications written in this program. This chapter is mainly about the practical work for this thesis. My PVSSII applications have been developed merely for training purposes, but have, nevertheless, a connection with the DCS for the SDD's power supply.

Chapter 2

ALICE experiment

2.1 Overview

In this chapter we briefly describe the detector complex ALICE (A Large Ion Collider Experiment) which is a general-purpose heavy-ion detector at the CERN LHC. It is designed [3, 4] to study quantum chromodynamics (QCD), the strong interaction sector of the standard model. The main goal of the ALICE is to study physical properties of the quark gluon plasma (QGP), possibly a state of matter that existed a few microseconds after the beginning of the universe. The detector was built by a collaboration including over 1000 physicists and engineers from 105 institutes in 30 countries.

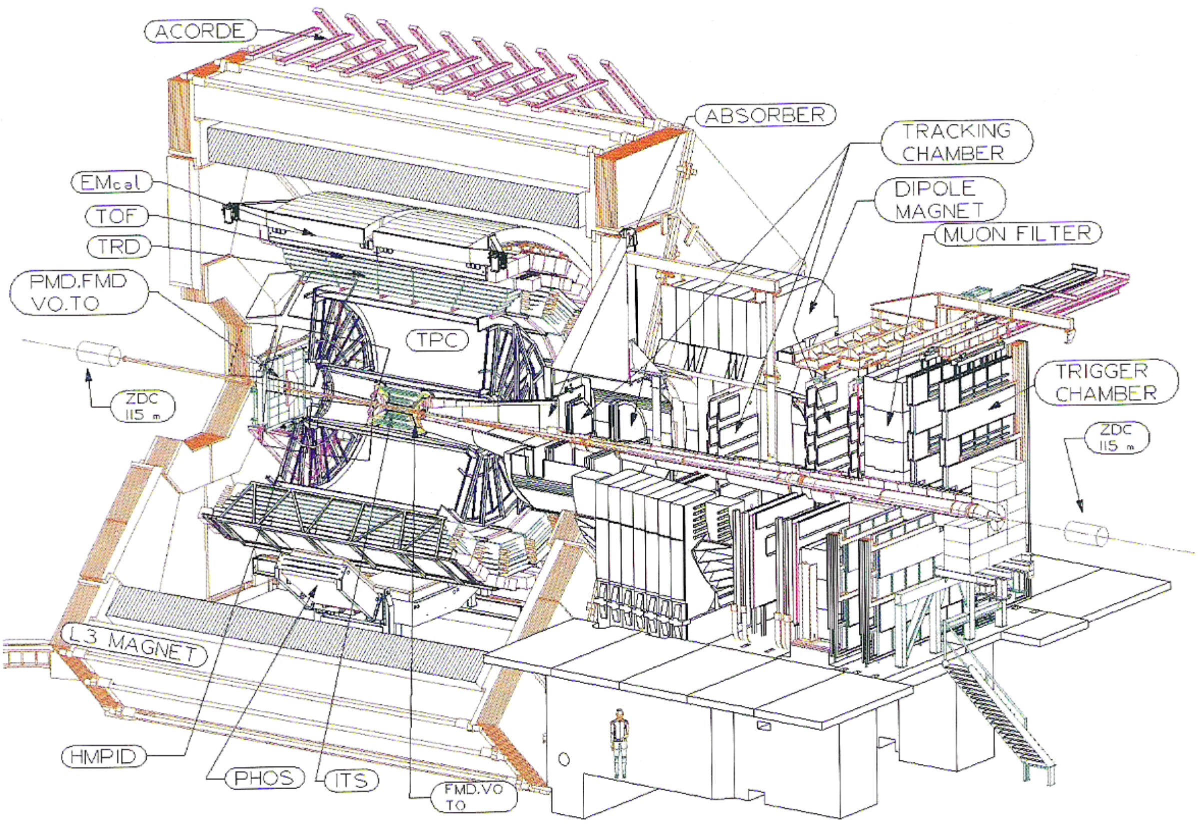

Figure 2.1: Overview of the ALICE detector [1].

The detector is composed of 18 sub-detectors and their associated supply systems [1, 2].

Table 2.1: Summary of the ALICE detector [1]. The acceptance in η is calculated from the estimated interaction point. The position is the approximate distance from the interaction point to the face of the detector and corresponds to the radius of the barrel detectors.

Detector	Acceptance (η, ϕ)	Position (m)	Dimension (m^2)	Channels
ITS layer 1,2 (SPD)	±2, ±1.4	0.039, 0.076	0.21	9.8 M
ITS layer 3,4 (SDD)	±0.9, ±0.9	0.150, 0.239	1.31	133 000
ITS layer 5,6 (SSD)	±0.97, ±0.97	0.380, 0.430	5.0	2.6 M
TPC	±0.9 at r=2.8 m	0.848, 2.466	readout 32.5 m^2	557 568
	±1.5 at r=1.4 m		Vol. 90 m^3	
TRD	±0.84	2.90, 3.68	716	1.2 M
TOF	±0.9	3.78	141	157 248
HMPID	±0.6, $1.2° < \phi < 58.8°$	5.0	11	161 280
PHOS	±0.12, $220° < \phi < 320°$	4.6	8.6	17 920
EMCal	±0.7, $80° < \phi < 187°$	4.36	44	12 672
ACORDE	±1.3, $60° < \phi < 60°$	8.5	43	120
Muon Spectrometer				
Tracking station 1	$-2.5 < \eta < -4.0$	-5.36	4.7	1.08 M
Tracking station 2		-6.86	7.9	
Tracking station 3		-9.83	14.4	
Tracking station 4		-12.92	26.5	
Tracking station 5		-14.22	41.8	
Trigger station 1	$-2.5 < \eta < -4.0$	-16.12	64.6	21 000
Trigger station 2		-17.12	73.1	
ZDC:ZN	$\lvert\eta\rvert < 8.8$	±116	2×0.0049	10
ZDC:ZP	$6.5 < \lvert\eta\rvert < 7.5$	±116	2×0.027	10
	$-9.7° < \phi < 9.7°$			
ZDC:ZEM	$4.8 < \eta < 5.7$,	7.25	2×0.0049	2
	$-16° < \phi < 16°$ and			
	$164° < \phi < 196°$			
PMD	$2.3 < \eta < 3.7$	3.64	2.59	2 221 184
FMD disc 1	$3.62 < \eta < 5.03$	inner: 3.2		
FMD disc 2	$1.7 < \eta < 3.68$	inner: 0.834	0.266	51 200
		outer: 0.752		
FMD disc 3	$-3.4 < \eta < -1.7$	inner: -0.628		
		outer: -0752		
V0A	$2.8 < \eta < 5.1$	3.4	0.548	32
V0C	$-1.7 < \eta < -3.7$	-0.897	0.315	32
T0A	$4.61 < \eta < 4.92$	3.75	0.0038	12
T0C	$-3.28 < \eta < -2.97$	-0.727	0.0038	12

Figure 2.1 summarizes the layout of ALICE. The table 2.1 shows details of the position of the detectors, and also the acceptance in pseudo-rapidity[1] η and the azimuthal angle ϕ.

The central part of the detector is barrel shaped and is situated in a solenoid magnet which is reused from the L3 experiment at LEP. The L3 magnet provides magnetic field of 0.5T.

From inside out, the barrel consists of Inner Tracking System (ITS), of six planes of high-resolution silicon pixel (SPD), drift (SDD), and strip (SSD) detectors, a cylindrical Time-Projection Chamber (TPC), three particle identification arrays of Time-of-Flight (TOF), Ring Imaging Cherenkov (HMPID) and Transition Radiation (TRD) detectors, and two electromagnetic calorimeters (PHOS and EMCal). All the sub-detectors except HMPID, PHOS, and EMCal cover the full azimuth.

The forward muon arm consists of several absorbers, a dipole magnet, and fourteen planes of triggering and tracking chambers. What is more, there are several smaller detectors situated in smaller angles (ZDC, PMD, FMD, T0, V0). An array of scintilators (ACORDE) is used for triggering of cosmic rays.

The detector is designed to withstand the highest multiplicities anticipated for Pb-Pb collisions which are extrapolated from RHIC and which were originally estimated to range from $\mathrm{d}N/\mathrm{d}\eta = 2000$ up to almost $\mathrm{d}N/\mathrm{d}\eta = 8000$. More recent extrapolations point to lower values of $\mathrm{d}N/\mathrm{d}\eta = 1500$–$4000$ [16]. The design of ALICE was optimized for the value of approximately $\mathrm{d}N/\mathrm{d}\eta = 4000$, but tested for simulations exceeding twice that amount.

Table 2.2: Doses and neutron fluences in central detectors [16].

System	Radius (cm)	Dose (Gy)	h-Φ (cm^{-2}) 1MeV n-equ
SPD1	3.9	2.7×10^3	3.5×10^{12}
SPD2	7.6	6.8×10^2	1.3×10^{12}
SDD1	14	2.5×10^2	5.5×10^{11}
SDD2	24	1.2×10^2	3.2×10^{11}
SSD1	40	5.0×10^1	2.3×10^{11}
SSD2	45	3.0×10^1	2.0×10^{11}
TPC(in)	78	1.6×10^1	1.5×10^{11}
TPC(out)	278	2.2×10^0	4.5×10^{10}
TRD	320	1.8×10^0	2.6×10^{10}
TOF	350	1.2×10^0	2.0×10^{10}
PHOS	460	5.0×10^{-1}	1.7×10^{10}
HMPID	460	5.0×10^{-1}	1.7×10^{10}

The radiation environment in the detector was simulated for the planned run scenario. Runs with p-p, low- and high-mass ion-ion collisions for over a ten year period were assumed. Moreover, beam-beam and beam-gas interactions, and miss-injected beams were expected as additional radiation source. Table 2.2 shows doses and neutron fluences for the central detectors.

2.2 Inner Tracking System (ITS)

This is the innermost group of detectors. The Inner Tracking System (ITS) [5] is composed of six layers of high resolution silicon detectors – two layers of silicon pixel detectors (SPD), two

[1] Pseudo-rapidity, quantity approximately equal to rapidity, is defined

$$\eta = -\ln \tan \frac{\theta}{2},$$

where θ is the longitudinal angle.

layers of silicon drift detectors (SDD), and two layers of silicon strip detector (SSD).

Its main purposes are to determine the primary vertex with a resolution less then 100μm, to reconstruct the secondary vertexes from the decays of hyperons and D and B mesons, to track and identify particles with momentum below 200MeV/c, to improve the momentum and angle resolution for the Time-Projection Chamber (TPC) and to reconstruct particles that cross the dead regions of TPC. The ITS will be described in more detail in chapter 4.

2.3 Time-Projection Chamber (TPC)

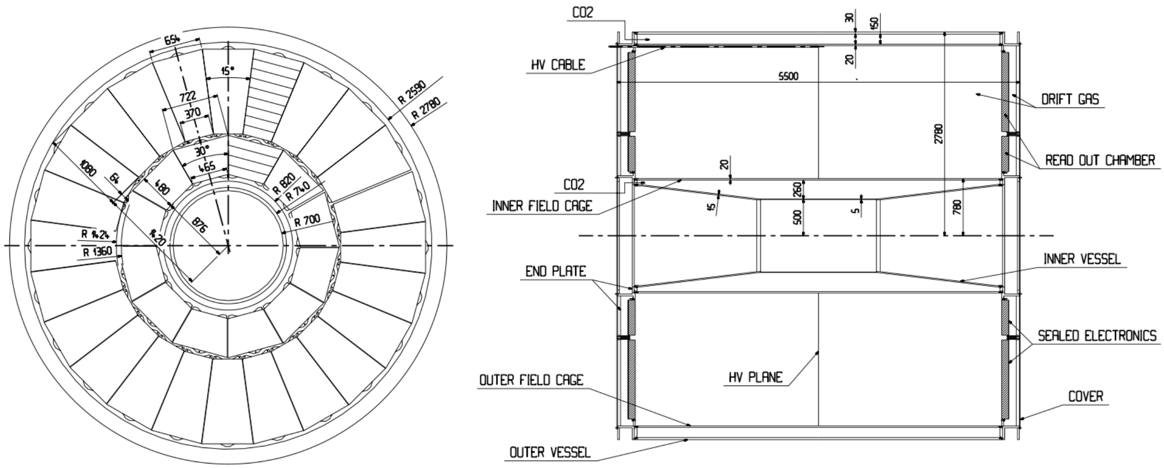

Figure 2.2: Schematic layout of the TPC [2]

The Time-Projection Chamber (TPC) is the main tracking detector of ALICE. The TPC is optimized to provide charged-particle measurements with good two-track separation, particle identification, and vertex localization. Moreover, data from the central barrel detectors are used for High-Level Trigger (HLT) that selects low cross section signals.

The detector is made of barrel shaped field cage (figure 2.2), filled with 90m^3 of Ne/CO_2/N_2 (90/10/5), in which the primary electrons are transported up to 2.5m on either side of the central electrode to the end plates. Multi-wire proportional chambers with cathode pad readout are mounted on 18 trapezoidal areas.

2.4 Transition Radiation Detector (TRD)

The main task for the Transition Radiation Detector is to provide electron identification for the momenta above 1GeV/c. Below this momentum the electrons can be detected by the TPC. For the momenta above 1GeV, specific radiation from the particles transferring a boundary between two media with different indexes of refraction, so called 'transition radiaton', can be measured.

The TRD significantly enhances the measurement of the Υ-yields, high-p_t J/ψ, the high mass part of dilepton continuum, as well as jets. Moreover, the TRD was designed to obtain a fast trigger for charged particles with high momenta. It is a part of the Level-1 trigger.

2.5 Particle IDentification (PID) system

Particle Identification (PID) system consists of two detectors – Time-Of-Flight (TOF) detector and High-Momentum Particle Identification Detector (HMPID).

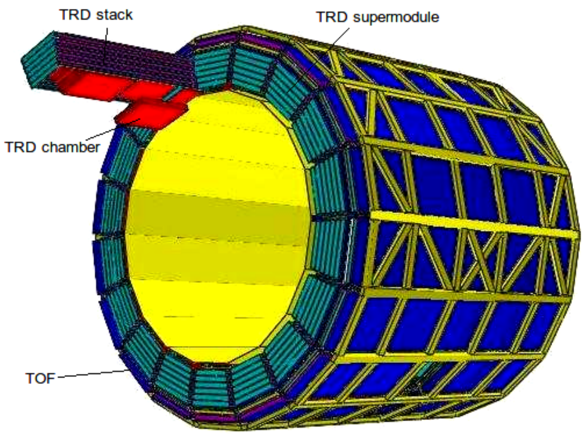

Figure 2.3: View of the TRD and the TOF layout in the ALICE space frame [1]. 18 super modules of the TRD each containing 30 readout chambers (red) arranged in 5 stacks of 6 layers are shown. One chamber has been displaced for clarity. Likewise, 18 super modules of the TOF (dark blue) are situated right above the TRD. Each super module of the TOF is divided into 5 modules.

2.5.1 Time-Of-Flight (TOF) detector

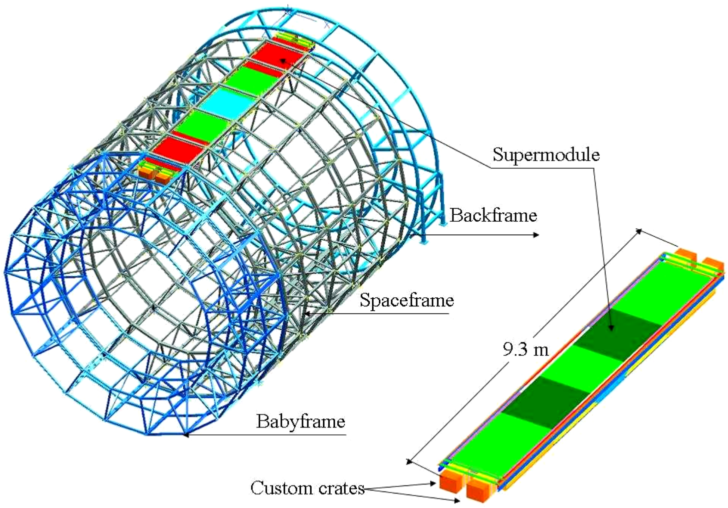

Figure 2.4: Schematic drawing of one TOF super module [1], consisting of five modules, in the ALICE spaceframe.

The Time-Of-Flight (TOF) detector is a large area array that covers the central pseudo-rapidities ($|\eta| \lesssim 0.9$) for PID in the intermediate momentum range. The TOF needs a very fast detection and since a large area has to be covered, the Multi-Gap Resistive-Plate Chamber (MRPC [19]) was chosen. There are over 10^5 channels of MRPCs in the TOF detector.

2.5.2 High-Momentum Particle Identification Detector (HMPID)

The High-Momentum Particle Identification Detector (HMPID) is aimed to enhance the PID capability of ALICE by enabling identification of charged hadrons beyond the momentum interval

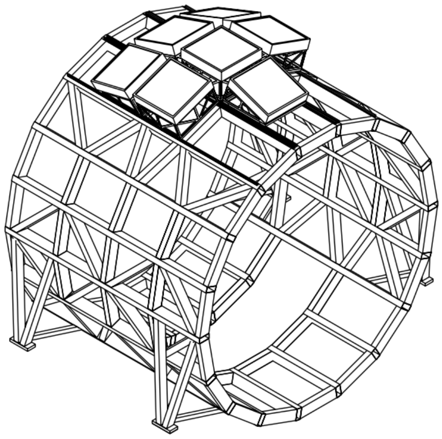

Figure 2.5: View of the HMPID assembled on the ALICE space frame [2].

measurable by ITS, TPS and TOF detectors. The HMPID is based on proximity-focusing Ring Imaging Cherenkov (RICH) counters [20] and consists of seven modules of about $1.5 \times 1.5\mathrm{m}^2$ each.

2.6 PHOton Spectrometer (PHOS)

The PHOton Spectrometer (PHOS) is a high-resolution electromagnetic spectrometer covering a limited acceptance at central rapidity. Its main objective is to measure prompt[2] photons, high-p_t π^0's and η's.

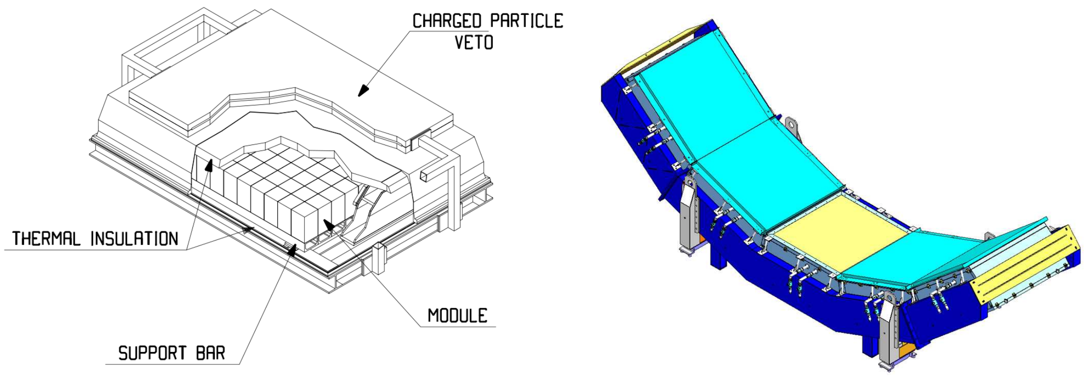

Figure 2.6: Detailed view of one PHOS module (on the left [2]) and drawing of the five PHOS modules (on the right [1]).

The layout of the PHOS is shown in figure 2.6. The PHOS consists of a highly segmented electromagnetic calorimeter (PHOS) and a Charged-Particle Veto (CPV) detector. It is subdivided into five independent PHOS+CPV modules. Each PHOS module consists of 3584 detection cells made of lead-tungstate crystal ($PbWO_4$) coupled to an Avalanche Photo-Diode (APD). To increase the efficiency of $PbWO_4$ crystals, the PHOS modules are operated at a temperature of -25°C. The CPV is a Multi-Wire Proportional Chamber with cathode-pad readout. Its charged-particle detection efficiency is better than 99%.

[2]Prompt photons are emitted directly from the collision and can reveal thermodynamic properties of the quark-gluon plasma.

2.7 ElectroMagnetic Calorimeter (EMCal)

The ElectroMagnetic Calorimeter (EMCal) is a large cylinder shaped Pb-scintillator sampling calorimeter. It is located approximately opposite in azimuth to the PHOS. The aim of EMCal is to study in detail the physics of jet quenching (interaction of energetic partons with dense matter). Moreover, EMCal provides a fast and efficient trigger (L0, L1, see section 2.11.1).

2.8 ALICE COsmic Ray DEtector (ACORDE)

ACORDE, the ALICE cosmic ray detector, is an array of plastic scintillator counters located on the top of the L3 magnet. It provides a fast trigger signal (L0) to filter the events that are in coincidence with cosmic rays. What is more, it also detects, in combination with TPC, TRD, and TOF, single atmospheric muons and multi-muon events thus allowing us to study cosmic rays in the energy region of the 'knee' in the cosmic spectrum.

2.9 Muon spectrometer

Muon spectrometer is mounted in the pseudo-rapidity region of $-4.0 < \eta < -2.5$. This detector measures the complete spectrum of heavy-quark vector-mesons resonances (i.e. J/ψ, ψ', Υ, Υ' and Υ''), as well as ϕ meson in the $\mu^+\mu^-$ decay channel. It also provides a very fast trigger (L0, L1).

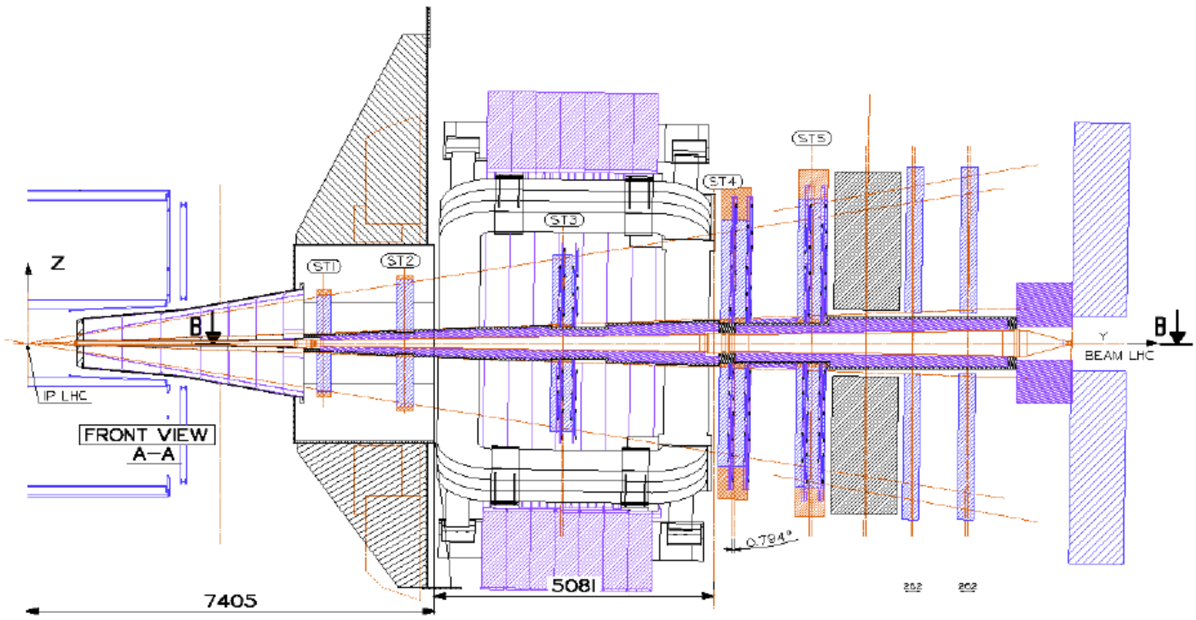

Figure 2.7: Muon spectrometer longitudinal section [1].

The layout of the muon spectrometer is shown in figure 2.7. The spectrometer consists of following components: a passive front absorber that absorbs hadrons and photons from the interaction vertex; a high-granularity tracking system of 10 detection planes; a large dipole magnet; a passive muon-filter wall, followed by four planes of trigger chambers; an inner beam shield to protect the chambers from particles produced at large rapidities. The detection planes are made of cathode pad chambers and are arranged in five stations: two before, one inside and two after the dipole magnet. Each station consists of two planes.

To separate low-p_t muons from the high-p_t ones the four trigger planes were installed behind a muon filter wall. Those planes are made of Resistive Plate Chambers operated in streamer mode [21] and are arranged by two into two stations about 1m from each other.

2.10 Forward detectors

Zero Degree Calorimeters (ZDC) The number of participant nucleons can be estimated by measuring the energy carried by non-interacting (spectator) nucleons. Two sets of hadronic ZDCs are placed outside the ALICE cave 116m from the Interaction Point (IP) on both sides. In addition, two small electromagnetic calorimeters (ZEM) are located at about 7m from the IP.

Photon Multiplicity Detector (PMD) measures the multiplicity and spatial ($\eta - \phi$) distribution of photons in the forward pseudo-rapidity region of $2.3 \leq \eta \leq 3.7$.

Forward Multiplicity Detector (FMD) The main functionality of the FMD is to provide charged-particle multiplicity information in the pseudo-rapidity range $-3.4 < \eta < -1.7$ and $1.7 < \eta < 5.0$. The FMD consists of three rings (FMD, FMD2 and FMD3) each consisting of inner and outer ring of silicon sensors.

V0 detector is a small angle detector consisting of two arrays of scintillator counters, called V0A and V0C, that are installed on both sides of the ALICE interaction point. V0 serves as an indicator of the centrality of the collisions and also provides a minimum bias trigger.

T0 detector was designed to agree with the following objectives: to generate a start time (T0) for the TOF detector with the precision of 50ps and to provide the earliest L0 trigger signals. The detector consists of two arrays of Cherenkov counters.

2.11 Triggers

2.11.1 Trigger system (TRG)

The first level of triggering of ALICE is performed by Central Trigger Processor (CTP) [6]. Its design was chosen to select events that suit the physics requirements and the restrictions set by the bandwidth of the Data Acquisition (DAQ) system, and the High Level Trigger (HLT).

The first data from the trigger have to be fast to satisfy the detector requirements. The fast part of the trigger has split up into two levels: a Level-0 (L0) signal, which reaches the detectors at 1.2μs, but is too fast to pick up all the trigger inputs, and a Level-1 (L1) signal, arriving at 6.5μs, which collects all the remaining fast signals.

The high multiplicities of Pb-Pb collisions make events that contain more than one central collision unreconstructable. Therefore, a final level of trigger (Level-2, L2) had to be implemented. This level of trigger waits 88μs to confirm that the event can be taken.

2.11.2 High-Level Trigger (HLT)

The simulation studies have predicted that the amount of data produced in TPC alone, in a single nucleus-nucleus collision, corresponds to about 75MB assuming $\mathrm{d}N_{\mathrm{ch}}/\mathrm{d}\eta = 8000$ at midrapidity [1]. The data rate for all detectors can easily reach 25GB/s, while the physics content might be small and the DAQ archiving rate is about 1GB/s. For this reason, the HLT's task is to select relevant events and to compress the data without loosing their physics content. The physics requirements of the HLT are:

Trigger Accept or reject events based on detailed analysis.

Select Select a physics region of interest within the event by performing only a partial readout.

Compress Reduce the event size without loss of physics information by applying compression algorithms on the accepted and selected data.

Chapter 3

Detector Control System (DCS)

3.1 Introduction

The main objective of the ALICE Detector Control System (DCS) [6, 7] is to ensure safe and correct operation of the ALICE experiment. It provides remote control in such a way that the whole ALICE experiment can be operated from a single workplace (ALICE Control Room – ACR at LHC point 2). The DCS was designed to reduce the downtime of the experiment, and therefore, contribute to high running efficiency. Although being developed by various groups in parallel, the DCS is a coherent and homogeneous system.

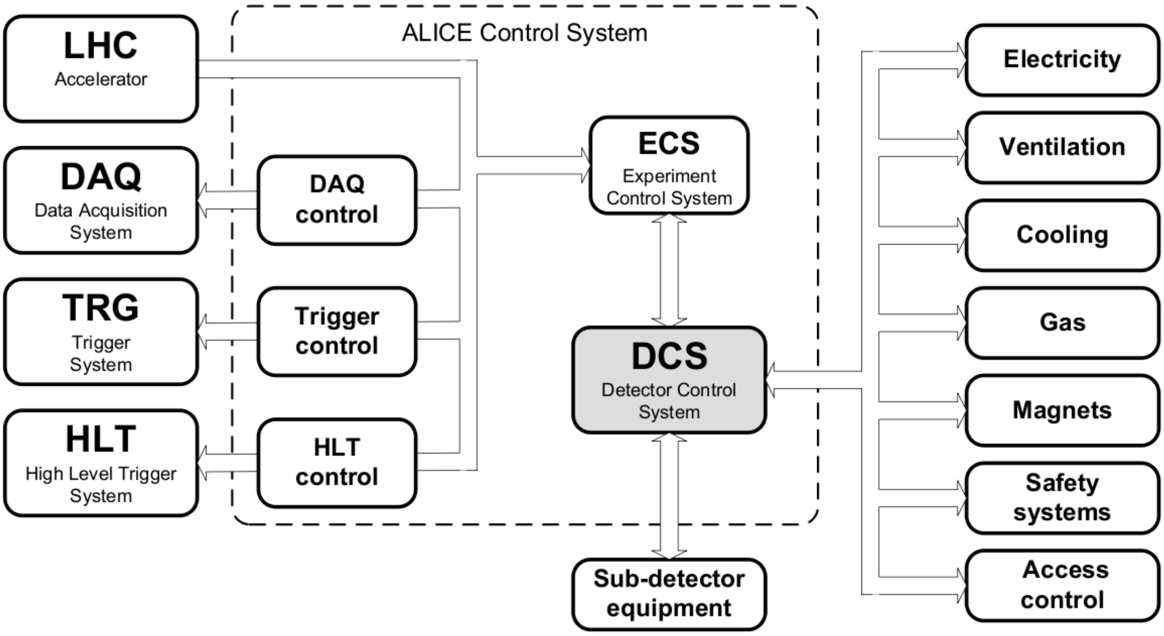

Figure 3.1: The ALICE online systems [6].

The DCS is a part of the ALICE Control System. As shown in figure 3.1, the ALICE Control System includes all control activities in the ALICE experiment: the Experiment Control System (ECS), the DCS, the Data Acquisition (DAQ), the TRG and the HLT (see section 2.11). The DCS takes care of interfering with the various services of the sub-detectors (such as cooling, electricity, magnets, safety, etc.). The ECS is responsible for the synchronization of the various systems, such as DCS, DAQ, TRG and HLT.

3.2 Requirements

The following design requirements were defined for the DCS:

Coherent and homogeneous Although the DCS covers a large number and a wide variety of devices, it must still be a coherent and homogeneous system across all the sub-detectors and sub-systems.

Flexible and scalable Since a lot of changes must take place during the lifetime of ALICE, the system has to be flexible enough to accommodate them. In addition, the DCS has to be operational during the installation of sub-detectors.

Operational modes and concurrent operation The DCS must be operational throughout all operation phases of the experiment; not just during data taking, but also during the shutdown periods. The DCS requirements can be different for various phases of the detector operation. Each sub-detector should be allowed some autonomy in the operation of its hardware. Therefore, each part of an experiment may be controlled independently to the rest of the experiment.

User friendly and intuitive operation Since the shift crew is not necessarily expert in controls or in operation of a detector, special attention was given to the presentation of the system to the operators.

Available, safe and reliable The DCS ensures the safety of the detectors, and is, therefore, required to be reliable and available (where needed, control equipment should be on safe power).

Remote access and types of users The control system allows remote access. Hence, a strict control mechanism, based on the origin of the user profile, has to be put in place for these accesses.

Configuration and archiving All relevant data for the operation of the experiment, as well as data needed for the configuring of the experiment equipment, are stored in databases.

Maintainable The system must be easily maintainable; this also when a part of the original expertise is no longer available.

3.3 System Architecture

3.3.1 Overview

The ALICE detector control system is responsible for configuring, monitoring and controlling the equipment of the experiment. This can be power supplies, but also specific devices for each sub-detector. It also controls computing devices and software running on them.

The DCS is designed to take preprogrammed decisions and automatic actions. Also, the operator can interact with the control system using the graphical user interface that presents the system and allows issuing of commands. To provide independent operation of any part of the equipment, the DCS is distributed over many computers in a transparent way.

3.3.2 Hardware Architecture

The hardware architecture is divided into three layers (see figure 3.2). The 'supervisory layer' is composed of PCs that provide user interfaces to the operators and are connected to the disk servers (that hold databases, archiving, etc.). The DCS also interferes with external systems through this layer via the DIP protocol (Data Interchange Protocol) which is a protocol defined in CERN that allows exchanging of information between various systems.

The supervisory layer interfaces to the 'control layer' mainly through a LAN. This layer also consists mainly of PCs that interface to the experimental equipment, but also of the PLCs[1] or PLC-like structures. These devices collect information from the lower, so called 'field', layer and make the detector equipment available for the supervisory layer. The control layer interfaces to the equipment in the field layer through fieldbuses[2], but also via the LAN.

The field layer contains all field devices (such as power supplies, fieldbus nodes, etc.), sensors and actuators, etc. It is designed to avoid sharing of devices between different sub-detectors so they can run simultaneously and concurrently.

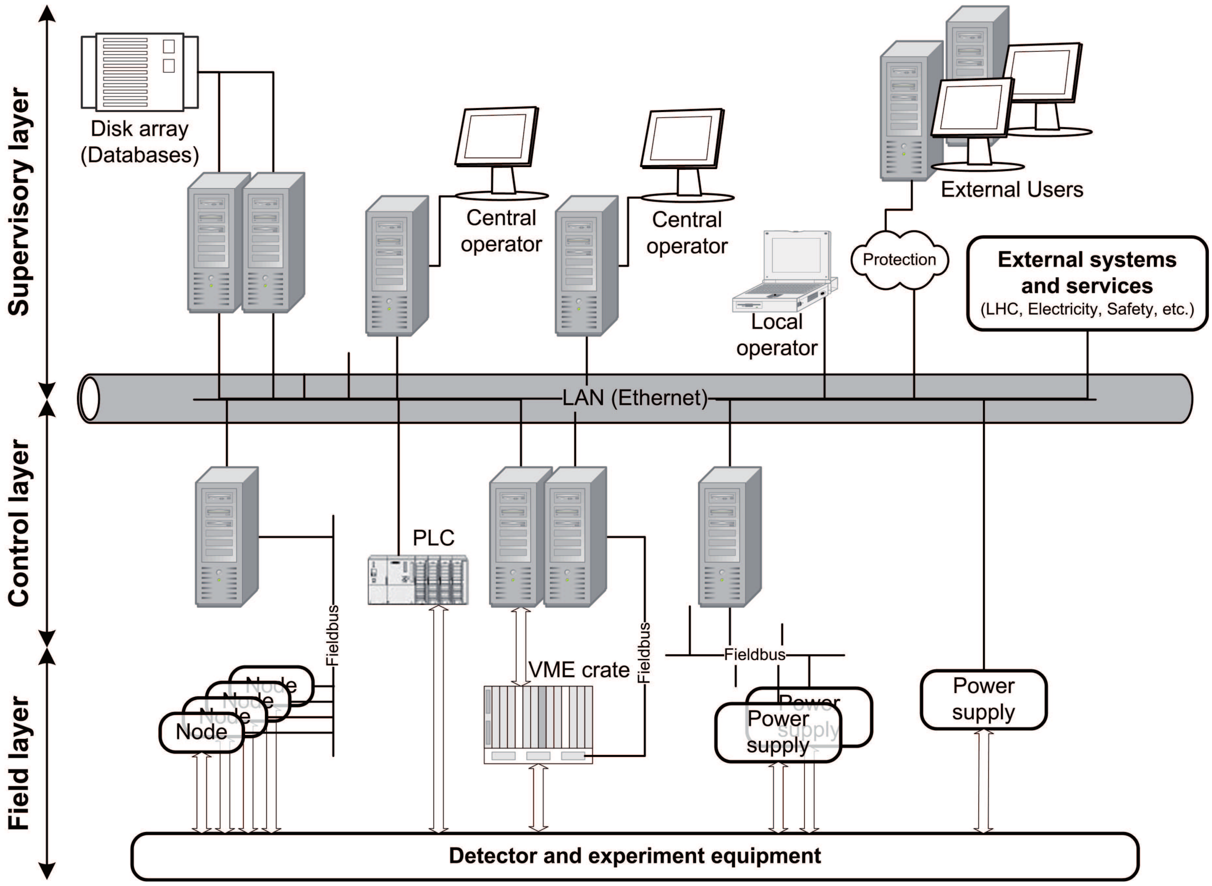

Figure 3.2: DCS hardware architecture [6].

3.3.3 Software Architecture

The software architecture is shown in figure 3.3. It is designed as a tree-like structure that represents the sub-detectors and their sub-systems and devices. Its structure is composed of

[1]PLC – Programmable Logic Controller is a computer used for automation of electromechanical devices, such as experimental equipment.

[2]Fieldbus is the name of industrial computer network protocols used for real-time distributed control. This network connects the PLCs to the experimental equipment.

nodes, each having a single parent except the top node, called the 'root node'. The node without children is called a 'leaf', and a subset of nodes is called a 'sub-tree'.

The nodes are sorted in three kinds: a Control Unit (CU), a Logical Unit (LU) and a Device Unit (DU). The control unit controls the sub-tree below, the device unit takes care of ('drives') a device, and the logical unit integrates several DUs in a group. This hierarchy provides a high degree of independence between the DCS components and allows for concurrent use.

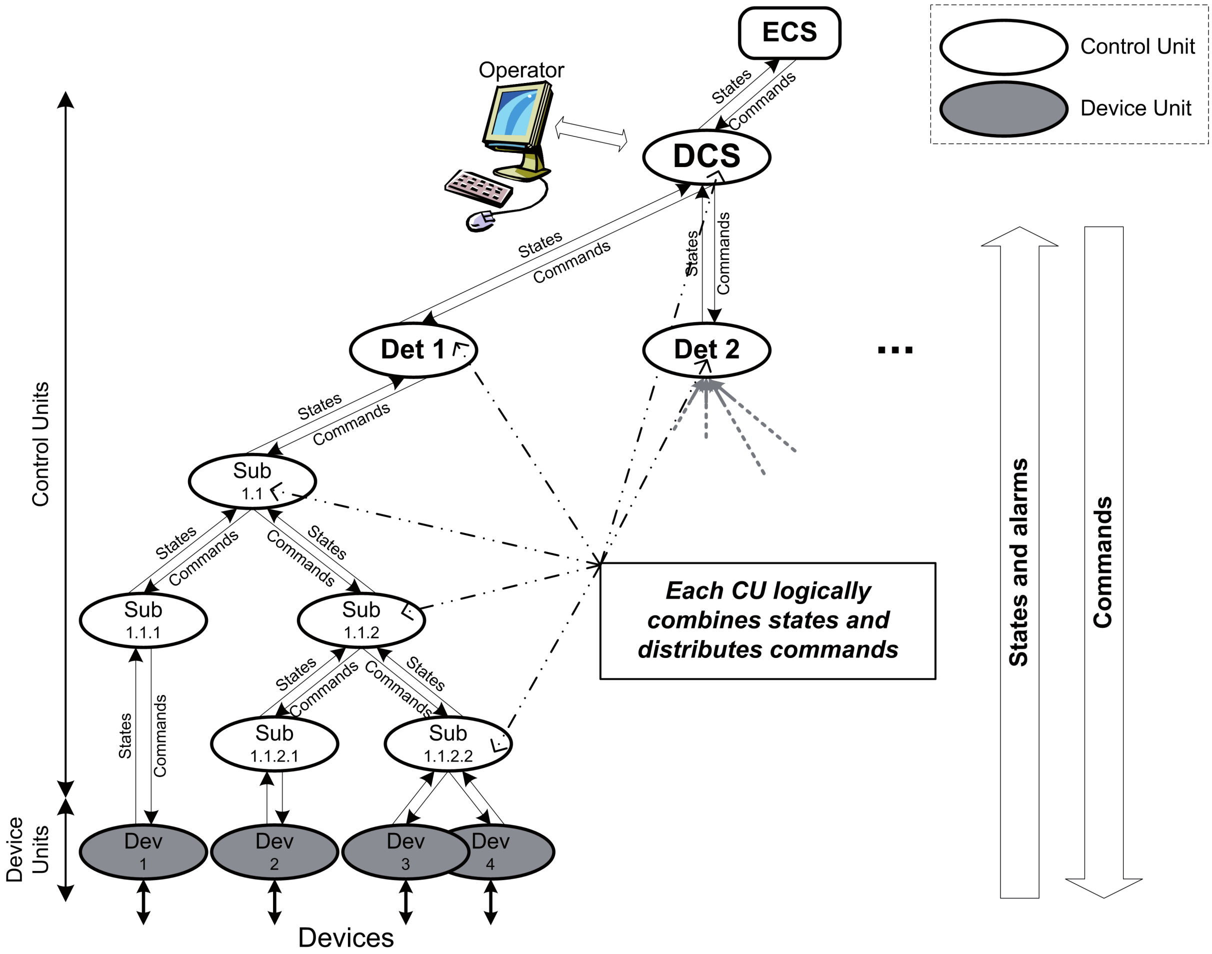

Figure 3.3: DCS hierarchical control architecture [6].

Each of the control and device units is responsible for configuration of itself and also of the tree below, and has a direct access to the configuration database. In addition, each unit is responsible for logging and archiving of the relevant data. Any device unit can generate alarms according to the received data from its associated device. As this alarm propagates upwards, each unit (including the first DU) reacts to this alarm in a preprogrammed way so the alarm avalanches are avoided.

The core software of the DCS is a commercial SCADA[3] (Supervisory Controls and Data Acquisition) program PVSSII [11].

The control system is built using the 'JCOP framework' which contains drivers for different types of hardware, communication protocols, and configurable components for frequently used applications such as low voltage power supply, etc. The framework also includes many other

[3]As the name indicates, SCADA (Supervisory Controls and Data Acquisition) are programs, designed to control and collect data from various hardware devices. They are not meant to be the full control systems, but focus on the supervisory level. As such, they are purely software products positioned on top of the hardware to which they are interfaced via PCs or PLCs [14].

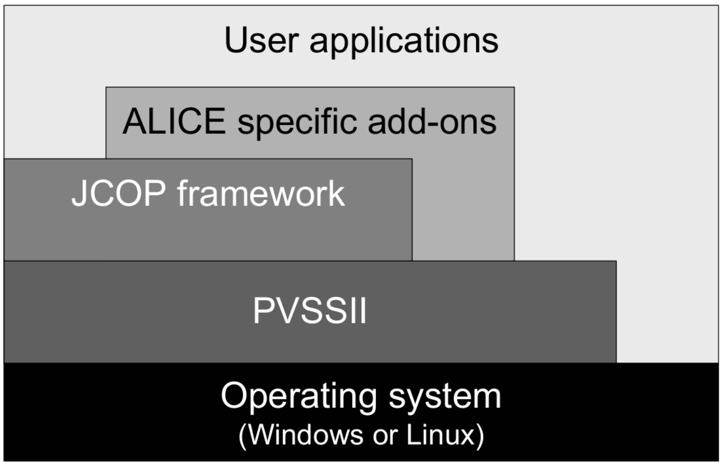

Figure 3.4: Overview of the software layers in the control system [6].

utilities such as interfaces to the various databases (configuration, archiving), visualization tools, access control, alarm configuration and reporting, etc. The JCOP framework is being developed by a joint effort between all the LHC experiments.

Several add-ons to this framework exist specially for the ALICE specific needs. The various layers are shown in figure 3.4.

PVSSII, the framework and the user applications are designed to work mainly on Microsoft Windows and Linux platforms. Some limitations, however, may exist for some Windows specific features, when using Linux.

Finite State Machine (FSM)

The hierarchical control structure is a tree-like structure composed of control units, logical units and device units. The units' behavior is modeled by the Finite State Machine (FSM) [13]. It is an intuitive, generic mechanism to program behavior of a piece of equipment or a sub-system. Every object in the FSM has a set of 'states' between which it can switch by performing 'actions' which are triggered by an operator or other components. There are two kinds of objects in the FSM: an abstract object and a physical object.

The abstract objects have a list of possible states and a list of allowed actions. An action consists of several instructions to the object. Possible instructions are also sent to other objects.

The physical objects are interfaced directly to the hardware. It receives commands from the piece of hardware it is connected to, and also from the abstract objects, and reacts to them by executing actions. These actions are programmed in standard languages such as C and C++ scripts, etc.

Control Units (CU)

Any node that has children is called a Control Unit. It models and controls the sub-tree below it. Its scheme is shown in figure 3.5. The behavior of the control unit can be modeled by the finite state machine concept. It reacts to the external commands (from its parent, children or the operator) by changing its state or sending commands to its children.

Device Units (DU)

Nodes without children (i.e. leaves) are called device units (DU). The DUs are responsible for controlling and monitoring of the associated devices. It receives commands from the operator or a parent node and translates them into commands for the device. It also collects data from

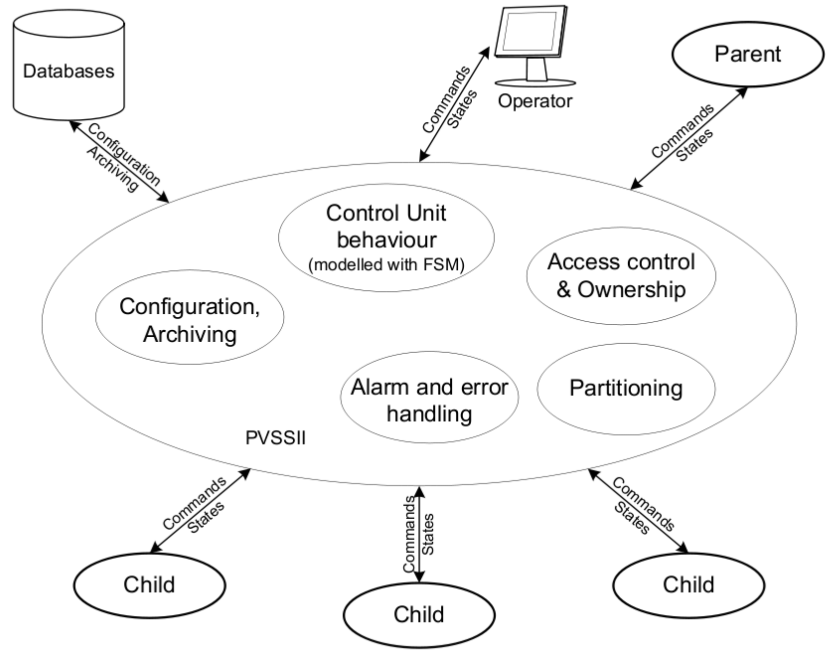

Figure 3.5: Functionality of a control unit [6].

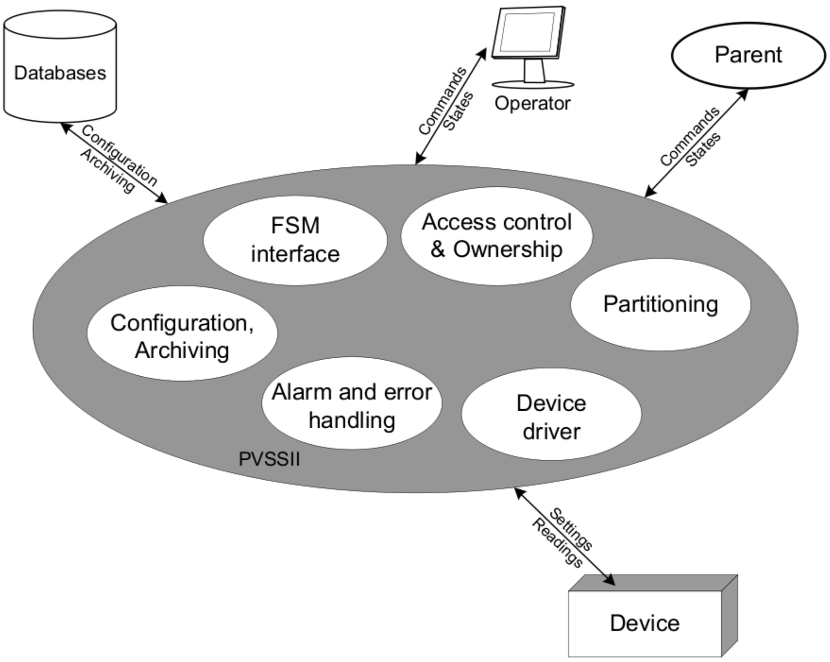

Figure 3.6: Functionality of a device unit [6].

the device and sends them to databases and its parent units. Unlike the CUs, no FSM logic is implemented in the device units. The DU contains all necessary drivers for the associated device and can, therefore, control it. Its functionality is explained in figure 3.6.

Logical Units (LU)

The Logical Unit (LU) is an object that can integrate several DUs; it can be enabled or disabled and cannot run in a stand-alone mode (cannot be partitioned off). It is useful at the bottom of the control tree for grouping the DUs. It behaves according to the state diagram and calculates its actions on the base of its children's states. A LU can integrate other LUs as well.

States and Commands

The communication between the nodes (control and device units) is done by a well defined, so called, states/commands system.

The commands propagate from the highest level down to the device units where they perform actions on the equipment. In each control unit, its state may change, if needed. The states propagate from the lower levels upwards. The device unit may response for the data read from the device by changing its state and sending its status to a parent control unit. The parent control unit can also react by changing its state to reflect this. This mechanism allows propagating of the data up to the highest level while correlating it with the other sub-trees. The whole mechanism is schematically drawn in figure 3.3.

Partitioning

Partitioning is the capability of controlling and monitoring a part of the system separately and concurrently from the rest of the system. This feature is essential during debugging and scaling of the control system, and also when a part of the detector is shut down but the rest is not.

Each part of the control tree, when declared as partitionable, can become a root node of a new control tree, and can be operated separately and concurrently from the rest of the system. Each node has a knowledge how to 'partition off' the rest of the control tree. The right to partitioning depends on the status of the system. The process of partitioning is shown in figure 3.7.

The PVSSII Program

PVSSII is the core software of the control system. It is a commercial SCADA system originally developed by the ETM company but it has been recently bought by Siemens. PVSSII is an object-oriented process visualization and control system that is used in industry and research. It is event-driven and designed as an distributed system. The tasks are performed by dedicated programs (so called managers) that can be distributed over various machines. The managers communicate through TCP/IP, and can run on both, Microsoft Windows and Linux. The PVSS itself does not support the FSM functionality so it has to be added, along with other features, by the JCOP framework.

The PVSSII is described in more detail in chapter 6. Moreover, my programs developed in PVSSII will be explained there.

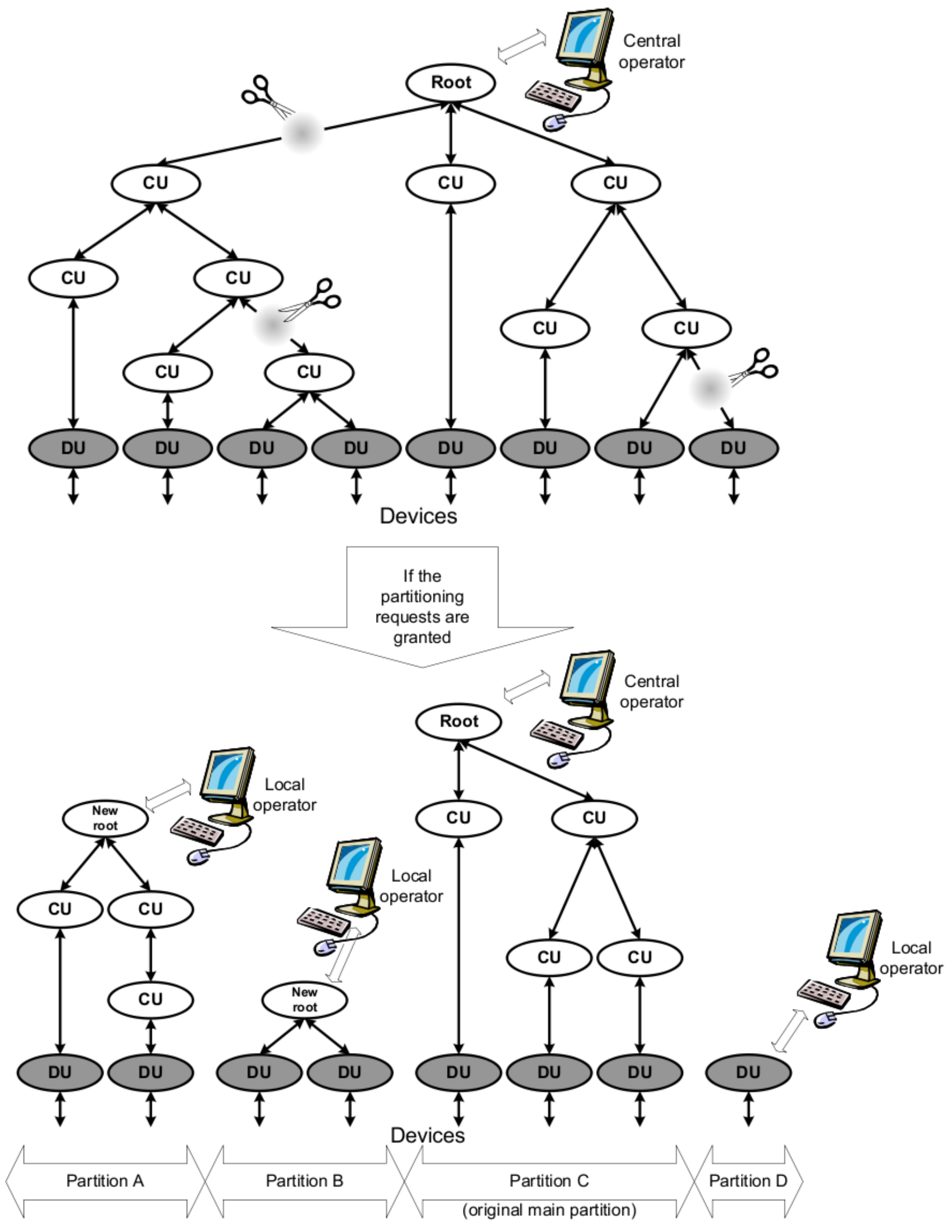

Figure 3.7: Partitioning [6].

Chapter 4

Inner Tracking System (ITS)

4.1 Overview

The Inner Tracking System (ITS) [1, 2, 5] is the closest detector to the beam pipe. Its main purposes are to localize the primary vertex and the secondary vertexes with a resolution better than 100μm, to track and identify particles with momentum below 200MeV, to improve the momentum and angle resolution of the TPC and to reconstruct particles that traverse dead regions of the TPC. The ITS also provides mechanical support for the beam pipe so it does not move during operation.

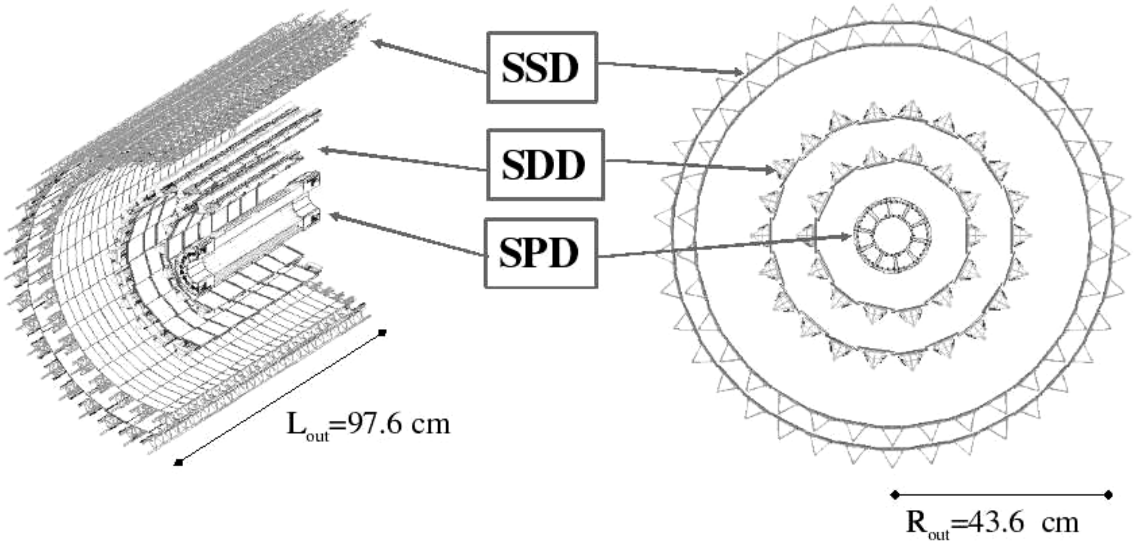

Figure 4.1: Layout of the ITS [1].

The ITS consists of six cylindrical layers of silicon detectors, coaxial with the beam pipe, as shown schematically in figure 4.1. It is located in radii between 4 and 43cm, and covers the pseudo-rapidity range of $|\eta| < 0.9$. The innermost layer of silicon pixel detector (SPD) has extended pseudo-rapidity coverage ($|\eta| < 1.98$) to provide, together with the FMD, continuous coverage for the measurement of the charged particles multiplicity. The dimensions of all the ITS detectors are summarized in table 4.1.

Because of the high particle density estimated in ion collisions at LHC (as many as 50 particles per cm^2 have been predicted for the innermost layer), and due to the fact that high resolution of the impact parameter is required, Silicon Pixel Detectors (SPD) have been chosen for the innermost two layers, and Silicon Drift Detectors (SDD) for the following two layers.

Table 4.1: Dimensions of the ITS detectors (active areas) [5].

Layer	Type	r (cm)	$\pm z$ (cm)	Area (m^2)	Channels
1	pixel	3.9	14.1	0.07	3 276 800
2	pixel	7.6	14.1	0.14	6 553 600
3	drift	15.0	22.2	0.42	43 008
4	drift	23.9	29.7	0.89	90 112
5	strip	38.0	43.1	2.20	1 148 928
6	strip	43.0	48.9	2.80	1 495 200
Total area				6.28	

Double sided Silicon micro-Strip Detectors (SSD) were installed on the two outer layers where the track density is expected to be below one particle per cm^2. The main parameters for each of the three detector types are shown in table 4.2. The detectors and front-end electronics are held by lightweight carbon-fiber structure (figure 4.2).

The four outer layers are equipped with analogue readout and can, therefore, be used for particle identification via dE/dx measurement in the non-relativistic ($1/\beta^2$) region. This feature gives the ITS stand-alone capacity as a low-p_t particle spectrometer.

Table 4.2: Parameters of the three detector types used in ITS [1]. A module represents a single sensor element. The maximum occupancy is calculated for the central Pb-Pb collisions.

Parameter		Silicon Pixel	Silicon Drift	Silicon Strip
Spatial precision $r\phi$	(μm)	12	35	20
Spatial precision z	(μm)	100	25	830
Two track resolution $r\phi$	(μm)	100	200	300
Two track resolution z	(μm)	850	600	2400
Cell size	(μm^2)	50×425	202×294	95×40000
Active area per module	(mm^2)	12.8×69.6	72.5×75.3	73×40
Readout channels per module		40960	2×256	2×768
Total number of modules		240	260	1698
Total number of readout channels	(k)	9835	133	2608
Total number of cells	(M)	9.84	23	2.6
Max. occupancy (inner layer)	(%)	2.1	2.5	4
Max. occupancy (outer layer)	(%)	0.6	1.0	3.3
Power dissipation in barrel	(W)	1350	1060	850
Power dissipation in end-cap	(W)	30	1750	1150

The granularity of the detectors was designed to cope with a track density of dN/d$\eta = 8000$, the upper limit of theoretical predictions. With this track density, the ITS would detect more than 15 000 tracks. The ITS detectors have a spatial resolution of the order of a few tens of μm, with the precision of 12μm for the detectors closest to the primary vertex. They, therefore, provide a resolution on the impact-parameter measurement adequate for heavy-flavored particle detection. The resolution is better than 60μm in the $r\phi$ plane for $p_\mathrm{t} > 1\mathrm{GeV}/c$). The spatial precision of the ITS is a crucial element of the momentum resolution for momenta above 3GeV$/c$.

The momentum and impact parameter resolution for low-momentum particles are dominated by multiple scattering effects in the material of the detector. Thus, the amount of material in densities for drifts and strips must have a minimum thickness of about 300μm to be able

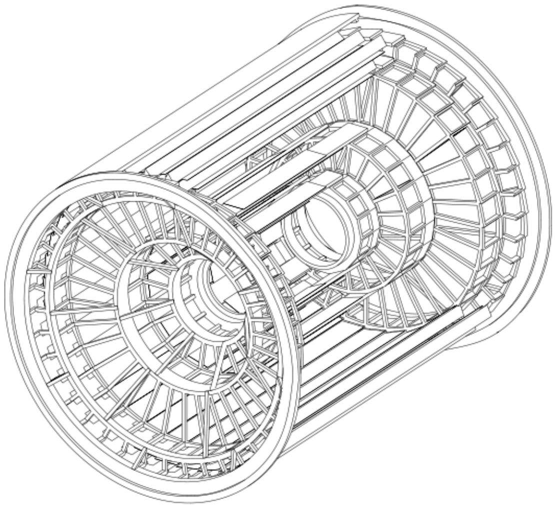

Figure 4.2: Schematic view of the mechanical support of the ITS [2].

Table 4.3: ITS material budget traversed by straight tracks perpendicularly to the detector surface [1]. Units are percentages of radiation length.

Detector	Pixel		Drift		Strip	
	Inner	Outer	Inner	Outer	Inner	Outer
Layer	1.14	1.14	1.13	1.26	0.83	0.86
Thermal shield/Support		0.52	0.25		0.53	
Total	7.18 (7.26 including air)					

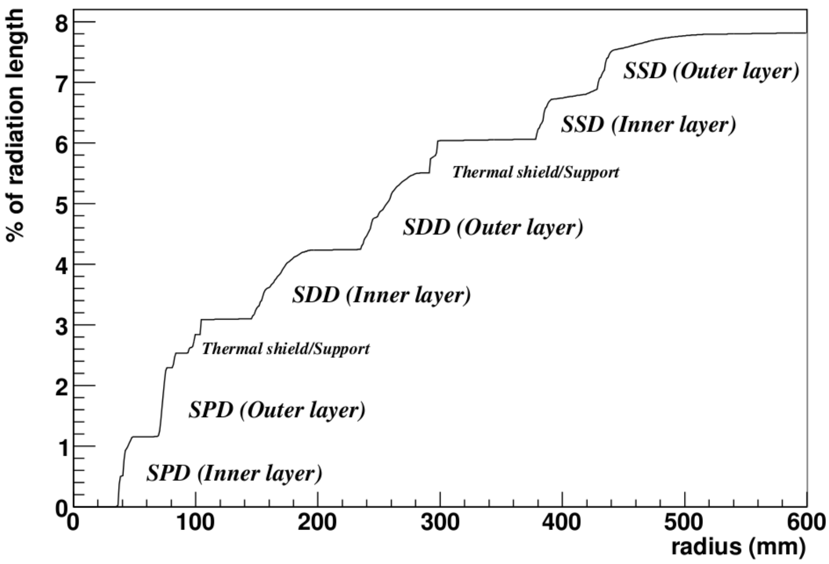

Figure 4.3: Plot of the integral of material thickness traversed by a perpendicular track originating at the primary vertex versus radius [1].

to provide acceptable signal-to-noise ratio. In addition, the detectors must overlap to avoid making of dead regions in the detector. The additional material in the active volume (i.e. electronics, cabling, support structure and cooling system) has been designed at comparable effective thickness (table 4.3 and figure 4.3).

For the ITS, the total dose expected during operation varies from tens of Gy for the outer parts to about 2.7kGy for the inner parts (see table 2.2 in section 2.1). All components of the ITS were tested for their radiation hardness to levels exceeding significantly the anticipated doses. The ITS is designed to withstand ten years of activity in the radiation environment.

Next, we briefly describe SPD and SSD layers. The SDD will be described in more detail in chapter 5 for it is the main topic of this thesis.

4.2 Silicon Pixel Detector (SPD)

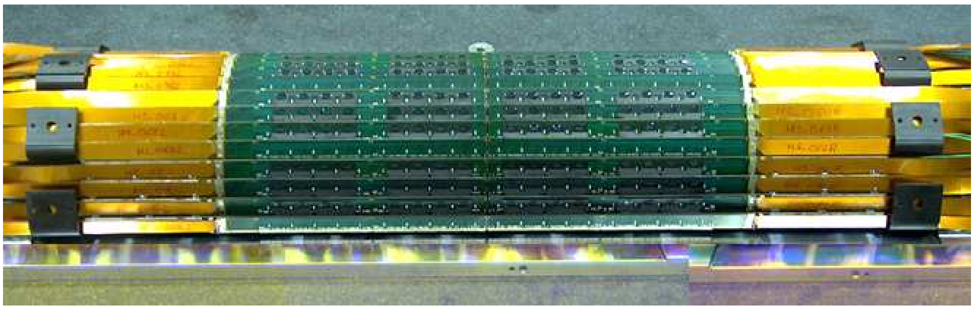

Figure 4.4: Half barrel of the SPD assembled on a reference table [1].

The Silicon Pixel Detector (SPD) composes the two innermost layers of the ITS. It operates in the region where the track density could reach 50cm^{-2}, and in relatively high radiation levels: for the inner layer, the total dose in ten year standard running scenario and fluence are estimated to be ≈2.7kGy and ≈3.5 $\times 10^{12}$n/cm^2 (1MeV neutron equivalent), respectively. The SPD is designed to minimize its material budget. The average material traversed by a straight track perpendicular to the detector surface is ≈1% X_0 per layer.

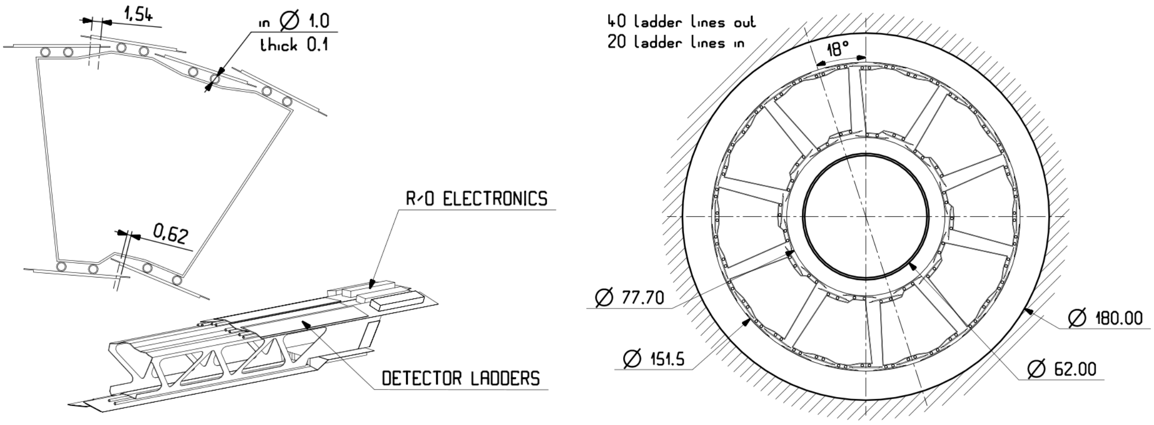

Figure 4.5: Left: view of a sector of the pixel barrel; right: cross-section of the pixel barrel [2].

The SPD is based on hybrid silicon pixels, consisting of two-dimensional matrix (sensor ladder) of reverse-biased silicon detector diodes bump-bonded to readout chips [22]. The readout is binary: the digital output level changes when a signal reaches a set threshold. The basic detector module is called half-stave. Each half-stave consists of two ladders and one readout chip (one Multi-Chip Module, MCM, and one high density aluminium/polyimide multi-layer interconnect). Each ladder is composed of a silicon sensor matrix bump-bonded to 5 front-end chips. The sensor matrix includes 256×160 cells measuring 50μm ($r\phi$) by 425μm (z).

Two half-staves are attached head-to-head along the z direction to a carbon-fiber support sector. Each sector supports six staves: two on the inner layer and four on the outer layer (see figure 4.5). In total, the SPD (60 staves) consists of 240 ladders with 1200 chips for a total of 9.8×10^6 cells.

The power generated by the front-end electronics is ≈1.35kW. The cooling system is of the evaporate type and is based on C_4F_{10}. In addition, the SPD barrel is surrounded by an Al-coated external shield to prevent heat radiation towards the SDD layers.

4.3 Silicon Strip Detector (SSD)

The Silicon Strip Detector (SSD) composes the two outermost layers of the ITS. Those layers are essential for matching of tracks from the TPC to the ITS. Moreover, they provide dE/dx information to assist particle identification for low-momentum particles. The particle density is estimated to be below 0.5cm^{-2}. Beam tests have shown that the spatial resolution is better than 20μm in the $r\phi$ direction and 820μm in the z direction.

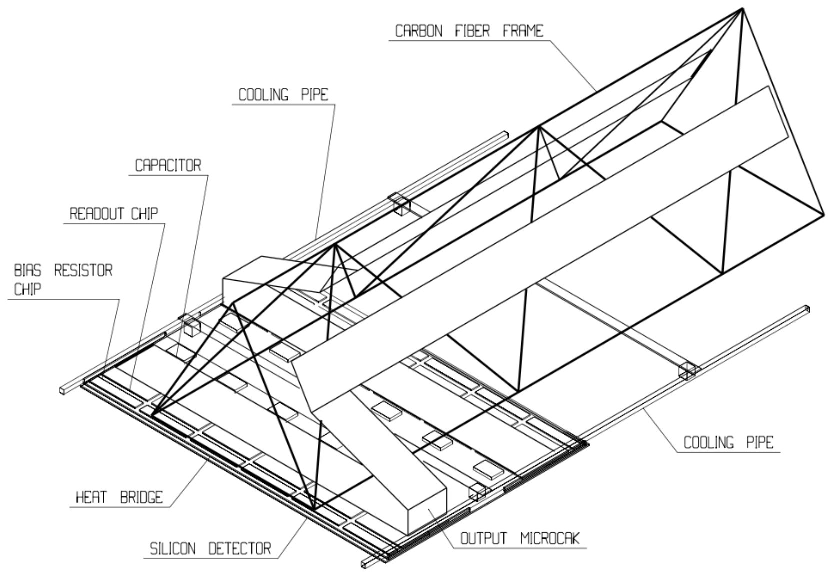

Figure 4.6: 3D view of one SSD module. The module shown here is glued on the carbon fiber ladder support [2].

Both layers use double sided SSDs, which have been chosen, because they introduce less material in the active area, compared to the single-sided SSDs. The detection modules are composed of one sector connected to two hybrids, one on the p-side and one on the n-side of the strips. All interconnections between the sensor and the electronics are made of aluminium on polyimide cables (micro-cables). The modules are assembled in ladders (figure 4.6), one module wide and up to 25 modules long. The 72 ladders, composed of 1698 modules, are mounted on a mechanical support structure in two concentric cylinders. For each layer, the ladders are mounted in two sightly different radii so they cover the full azimuth.

The sensors are 300μm thick and have 768 strips on each side with a pitch of 95μm. The stereoscopic angle is 35mrad (see figure 4.7) which is a compromise between stereo view and

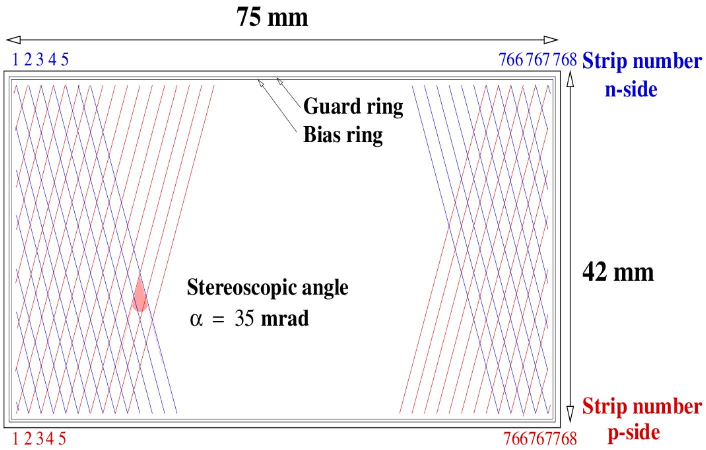

Figure 4.7: Scheme of a part of the SSD. Some characteristic dimensions are indicated [5].

reduction of ambiguities from high particle densities. The sensors are mounted with strips nearly parallel to the magnetic field in order to optimize the resolution in bending direction.

The mechanical support structure is made of carbon fiber composite, thus reducing the material budget. The average power dissipated in the barrel is ≈2.2kW. The cooling system is also designed to introduce minimum material, and to agree with the zero heat balance required for all ALICE detectors. Water was chosen as the cooling medium.

Chapter 5

Silicon Drift Detector (SDD)

5.1 Overview

The Silicon Drift Detectors (SDD) [1, 5, 24] make the two intermediate layers of the ITS in which the particle density is expected to reach 7cm^{-2}. They were chosen for their very good multi-track capability and because they provide, along with the silicon strip layers, two out of four dE/dx samples needed for the ITS particle identification.

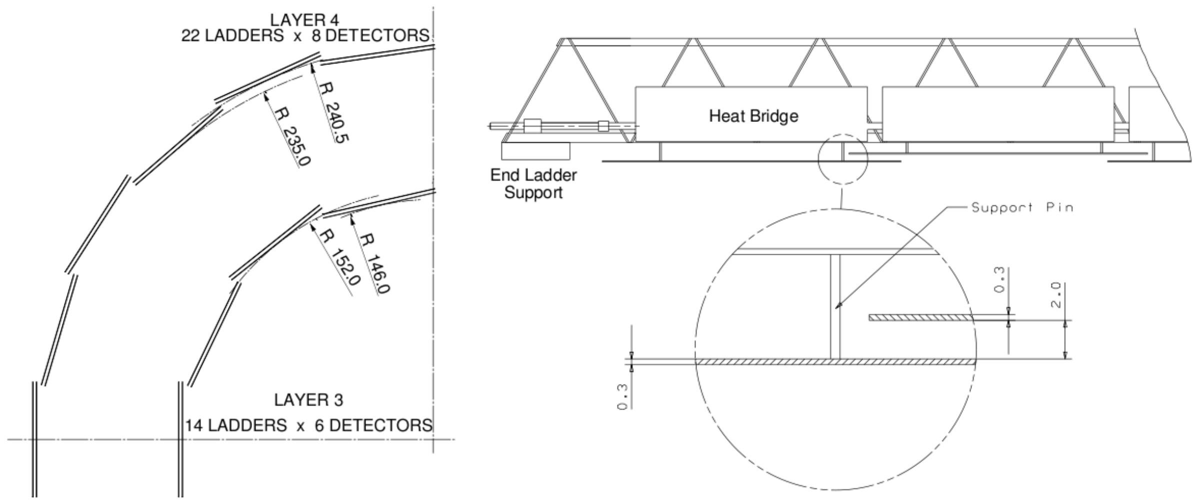

Figure 5.1: Schematic view of the SDD layers [1]. The SDD modules are mounted at different radii at both z and $r\phi$ planes to obtain the full coverage in the acceptance region.

In the drift detectors, the detection is made by measuring the transport time of charge, released during traversing of a particle at a certain spot, and reconstructing (in one dimension) this spot. The SDDs provide very high resolution at the cost of the readout speed (a few μs).

The two SDD layers are divided into 260 modules, each consisting of one silicon drift detector and two front end hybrids, connected to an end-ladder LV board (see fig. 5.5). The modules are mounted on linear structures called ladders. There are 14 ladders with six modules each on layer 3, and 22 ladders with eight modules each on layer 4. The ladder space frame is made of carbon-fiber reinforced plastic and has a protective coating against humidity. The layout of the SDD layers is shown in figure 5.1.

The ALICE SDDs were built out of very homogeneous high-resistivity (3kΩcm) 300μm thick Neutron Transmutation Doped (NTD) silicon. As shown in figure 5.2, the SDDs have a total area of 72.50($r\phi$)×87.59(z)mm^2 and a sensor area of 70.17×75.26mm^2. The sensitive area is divided

Table 5.1: Main parameters of the ALICE SDD layers and ladders [1].

	layer 3	layer 4
Detectors per ladder	6	8
Ladders per layer	14	22
Detectors per layer	84	176
Ladder sensitive half-length (cm)	22.16	29.64
Average ladder radius (cm)	15.03	23.91
Ladder space-frame weight (g)	11	15
Weight of ladder components (g)	87	121

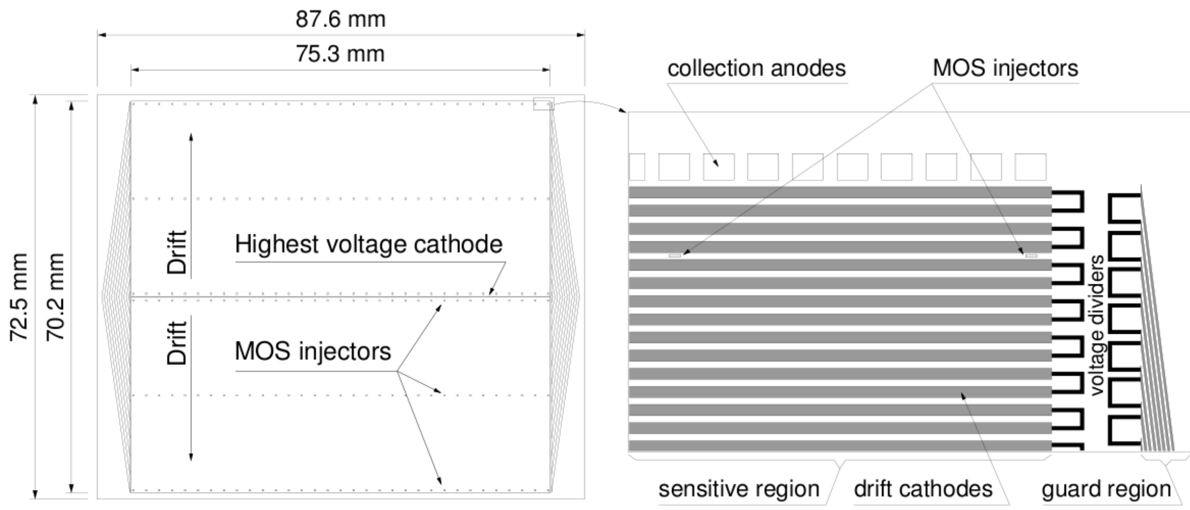

Figure 5.2: Layout of the ALICE SDD [1]. The detecting area is split into two 'drift regions' by the central cathode with the highest voltage. Each drift region has one row of 256 collection anodes and three rows of 33 MOS charge injectors for monitoring the drift velocity. Drift and guard regions have independent voltage dividers.

into two drift regions by the central cathode strip to which a high-voltage bias of −2.4kV is applied. A second bias supply of −40V is added to keep the biasing of the collection independent on the drift voltage. The detector performance, when averaged throughout its whole area, does not depend significantly on the applied bias voltage in a range from −1.65kV to −2.4kV, so the bias voltage can be adapted to the specific running conditions. The main characteristics of the SDDs are summarized in tables 5.2, and 4.2 on page 30.

5.2 Calibration

Drift velocity depends on mobility[1] which depends very strongly on temperature ($\mu \propto T^{-2.4}$), thus every module has a different drift speed. The temperature has to be controlled with precision ≈0.1K.

[1]Mobility μ characterizes how quickly an electron or a hole can move through a material, when pulled by an electric field. It is defined

$$v_d = \mu E \,,$$

where v_d is the drift velocity and E is the applied electric field.

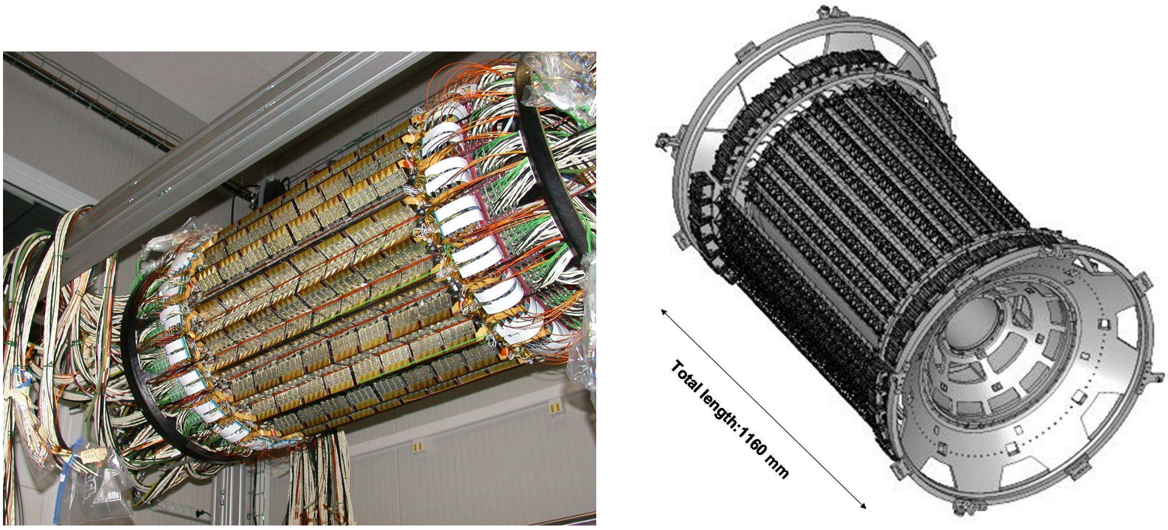

Figure 5.3: Left: the SDD completely assembled, ready to be integrated with the Silicon Strips. Right: A 3D image of the SDD layers, showing the support cones and the ladders of the two layers [1].

Table 5.2: The main characteristics of the ALICE silicon drift detectors [1].

Sensitive area	70.17×75.26mm^2
Total area	72.50×87.59mm^2
Collection anodes (readout channels)	2×256
Anode pitch	294μm
Operating voltage	-1.65 to -2.4kV
Nominal bias of the collection region	-40V
Drift velocity	5.6 to 8.1μm/ns
Maximum drift time	4.3 to 6.3μs
Cell size at drift velocity 8.1μm/ns	294×202μm^2
Cells per detector at drift velocity 8.1μm/ns	2×256×174
Total number of cells (266 SDDs)	23×10^6
Average resolution along the drift ($r\phi$)	35μm
Average resolution along the drift (z)	25μm
Detection efficiency	99.5%
Average double-track resolution at 70% efficiency at max. field	700μm

In order to monitor the drift velocity, so called MOS injectors were installed. They introduce the charge on known positions, thus allowing the drift speed to be measured. Every ≈6 hours (in future this should be improved to ≈10 min during physics runs), special runs take place to calibrate the drift speed [26].

5.3 Front-end electronics and readout (FERO)

The SDD front-end electronics consists basically of three types of ASICs[2]. The first two, PASCAL and AMBRA, are mounted on the front-end hybrid. PASCAL consists of three blocks:

[2]ASIC – Application-Specific Integrated Circuit is an integrated circuit suited for a particular use, rather than a general use. For example, a chip designed solely to run a cell-phone is an ASIC.

preamplifier, analogue storage and Analogue-to-Digital Converter (ADC). AMBRA, which receives data from PASCAL, performs data derandomisation and compression. The AMBRA also sends data to the third ASIC, CARLOS, which is a zero-suppressor, and also compresses data. In CARLOS, which is placed on the end-ladder structure (see fig. 5.6), the data is compressed from the raw 24.4MB by more than one order of magnitude. The CARLOS also provides a control interface via the JTAG[3] protocol. The CARLOS chips are connected with the DCS via I^2C using the mini-coaxial cables (more on that subject later). The front-end electronics assembly is shown in figure 5.4.

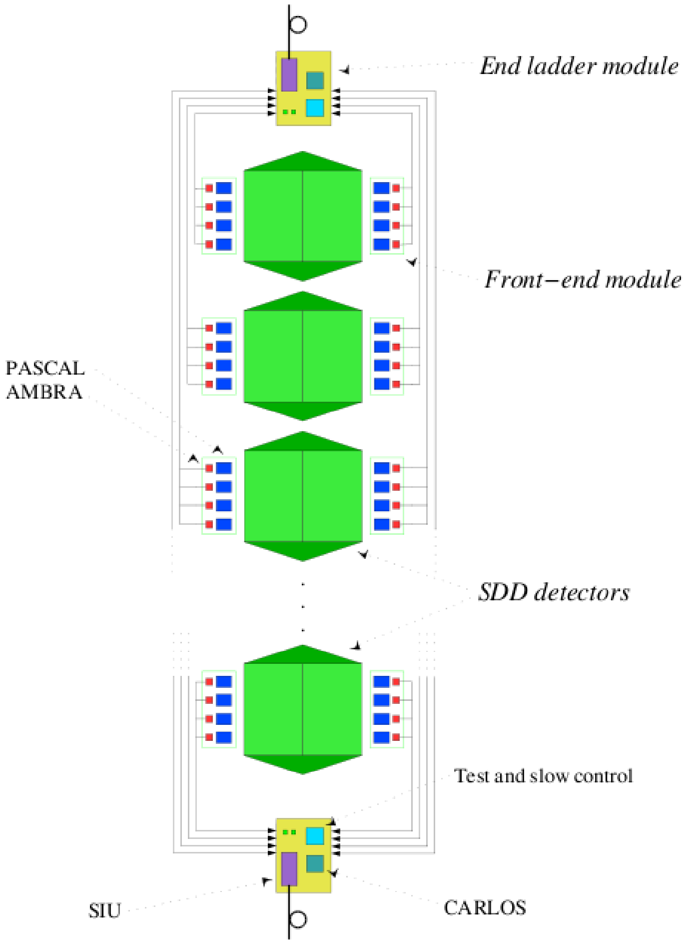

Figure 5.4: The SDD ladder readout scheme [5].

The SDD data readout works as follows:

1. The signal from SDD anode feeds the PASCAL. The SDD is still in the 'IDLE' state.

2. After receiving the L0-trigger signal, the 'BUSY' status is set immediately. After a programmable delay which accounts for the L0 latency (1.2μs) and the maximum drift time ($\approx 5\mu$s), the analogue memories are frozen.

3. The BUSY being still set, the data are digitalized by the PASCAL's ADCs and written to one of the free AMBRA's buffers.

[3]JTAG is an abbreviation of the Joined Test Action Group which has developed this protocol. The JTAG protocol is one of the standard means of connecting of the hardware devices to the DCS.

4. The digitalization lasts about 230μs and can be aborted by the absence of the L1 trigger or by the arrival of the L2-reject signal. In both cases, the front-end electronics resets the BUSY signal and returns to the IDLE state.

5. When the conversion is completed, all the AMBRAs transmit the data in parallel to the CARLOS chips on the end-ladder. This takes ≈1.23ms.

6. The CARLOS chips reduce the size of the data and format them in order to feed GOL (Gigabit Optical Link) ASICs which drive the optical links to the counting room.

7. In the counting room, 24 VME[4] boards concentrate the data from the 260 SDDs into 24 DDL (Detector Data Link) channels and feed the DAQ servers.

5.4 Power supplies

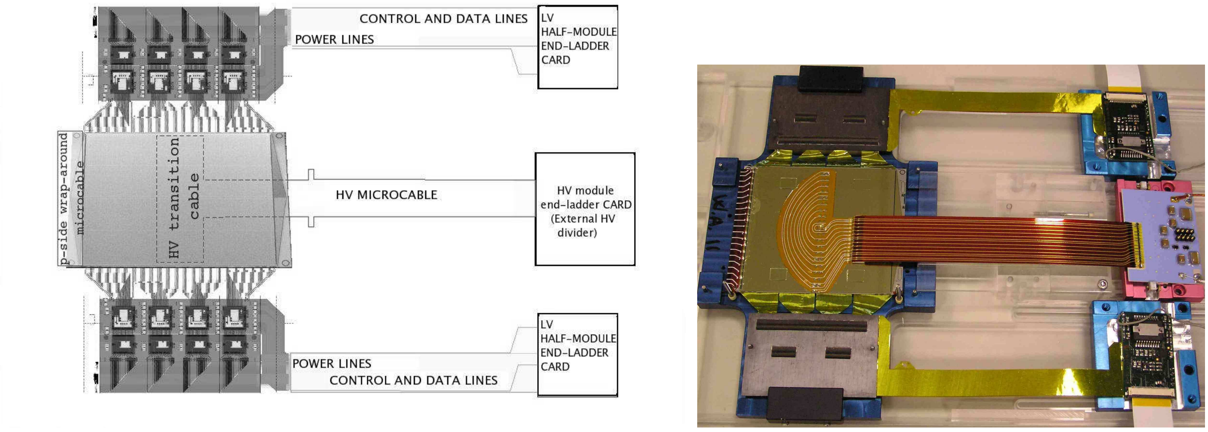

Figure 5.5: Scheme (left) and a photograph (right) of a SDD module [1].

The two front-end ASICs are connected to the corresponding end-ladder LV boards. The detector bias voltage is provided by specially designed printed circuit, called "micro-cables" which can carry high-voltage up to 2.4kV and connect the detectors to the HV end-ladder boards.

The connections to the central bias cathode and to the injector line are provided by a micro-cable, glued to the p-side. The bias lines are wire bonded to the corresponding bonding pads. The high-voltage is then brought to the n-side using the so called 'wrap-around' cable. These cables are clearly visible in figure 5.5.

The LV boards ensure the signal interfaces and low-voltage distribution, carry the low-voltage regulators, the circuitry to drive the MOS injectors and the interface with the DCS. The HV boards carry the support high-voltage divider. The end ladder boards are connected to the DCS via mini coaxial cables.

5.5 Cooling

Although the MOS injectors have proven to be an excellent monitoring instrument of the drift velocity, the cooling system has been designed with extreme care to provide a temperature stability of less than 0.1K. The cooling system is composed of a combination of two independent

[4]VME – Versa Module Eurocard is a computer bus standard.

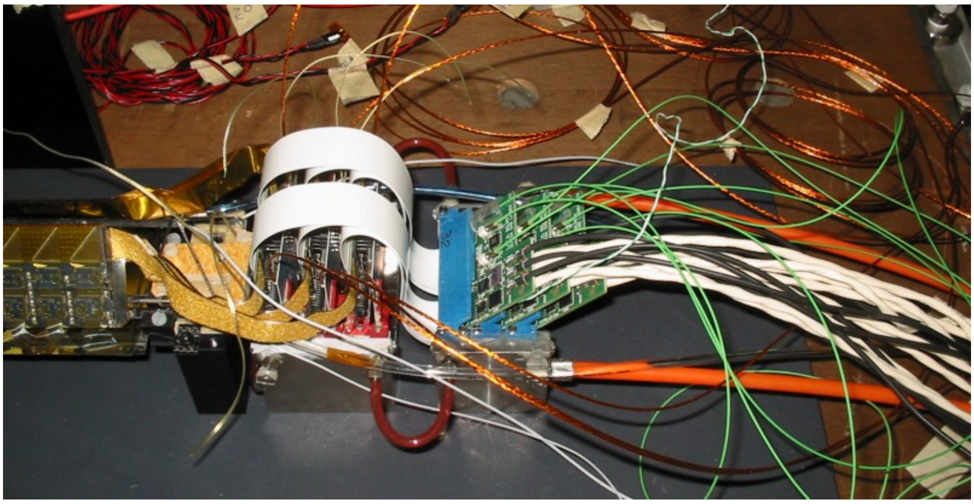

Figure 5.6: Detail of the end-ladder structure [8]. The CARLOS boards are on the right and are connected to LV boards with the flat white cable. HV boards are next to the LV (the thin orange cable supplies HV). The gold micro-cables connects the ladder electronics with the end-ladder and supplies chips with LV. The wires connected to the CARLOS are: white LV cables, black I^2C cables (see section 5.6.1) and green optical fibers to the DAQ.

under-pressure water circuits, filled with demineralized water: one coupled with the front-end electronics via pipes running along the ladder structure, and the second one coupled to the read-out electronics, LV and HV boards via pipes embedded to the end-ladder structure. Depending on its position, a cooling circuit cools two or four ladders and the related end-ladders. The water cooling is complemented by a moderate air flow preventing the creation of the hot spots and providing additional cooling to the sensors.

To ensure proper operation of the cooling circuits, each of the 13 cooling circuits is controlled by four pressure regulators and monitored by four flow-meters and six pressure sensors.

5.6 DCS structure

5.6.1 DCS electronics

The ladders' slow control [8] is provided by two types of DCS chips: DILBERT is a control chip responsible for the enabling/disabling of the other DCS and DAQ chips, and also for transforming the specific I^2C bus[5] communication (more on this subject below) into the standard form; the second DCU2 (Detector Control Unit) chips are 8-channels 12-bit ADCs, designed to provide information about voltages, currents and temperatures. There are always one DILBERT and three DCUs dedicated to control one module and its electronics. The DILBERT chip and one DCU are located on the CARLOS chip, and two DCUs are on left and right LV-boards (figure 5.7). The DILBERT is connected to the DCUs via standard I^2C bus using the JTAG protocol.

The DILBERT chip is connected to the, so called, DCS board, however the average distance between the DILBERT and the DCS board is approximately 5m. Therefore, the connection between them could not be done via standardized I^2C connection which is not suited for long connections in a noisy environment. Thus, a somewhat modified differential I^2C bus had to be implemented. Using this connection, four SDD modules can be connected to one DCS board.

[5] 'I^2C' is an abbreviation of 'inter-integrated circuit' and is a standard two-wire computer bus that is used for connecting low-speed peripherals to the motherboards or other embedded systems.

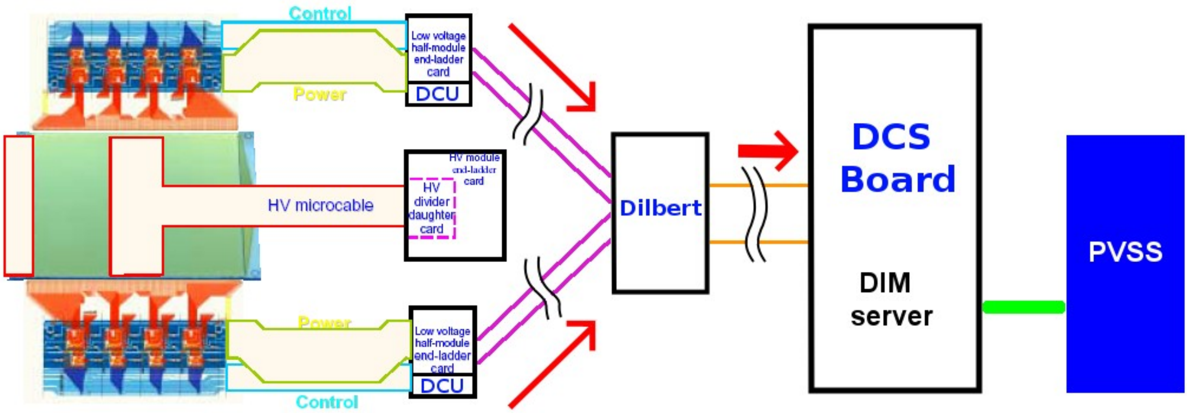

Figure 5.7: SDD control scheme [8].

The DCS board used for the SDDs is common to multiple detectors in ALICE. It is based on a Field-Programmable Gate Array[6] (FPGA) combined with an embedded computer solution. It runs on a minimalistic Linux distribution. The board hosts a significant portion of the front-end DCS. At this place, the logical commands are translated into the real hardware actions.

Once the low-level communication is taken care of, a need for a device, that would collect the data from the DCS board and distribute them to the SCADA, arises. For this purpose, the CERN developed DIM (Distributed Information Management) system is used. DIM is a light weight and high performance solution alternative to the industrial OPC[7] standard running only on the Microsoft Windows OS.

5.6.2 The FSM tree

The finite state machine structure (so called FSM tree) is shown in figure 5.8. The FSM tree [7] is naturally divided by three main control units: 'Layer 3 and 4' CUs which control the front-end electronics and readout (FERO) and the end-ladder controllers of the power supply, and the 'Infrastructure' CU that controls the cooling, the VME boards and the power supply. The infrastructure CUs have to be separated because they are not structured into similar sectors as the detector modules. For example, one FERO power supply channel feeds several FERO chips.

The figure 5.8 is from the year 2008 and the FSM tree has changed since then. For instance, every SDD module has its own CU. In the future, the FSM structure will change even more significantly because the SDD control system is going to be integrated under the ITS control system.

[6] Field-Programmable Gate Array (FPGA) is an integrated circuit designed to be configured by a customer or designer after manufacturing. Hence, it is truly field-programmable. The FPGAs can be used to implement any logic operations that an ASIC could perform. The ability to update its functionality after shipping, however, offers many advantages for many applications.

[7] The Object Linking and Embedding for Process Control (OPC) standards [15] specify the solutions for the communication of the industrial devices. They define the standards for the device data accesses, alarms and events, security, etc.

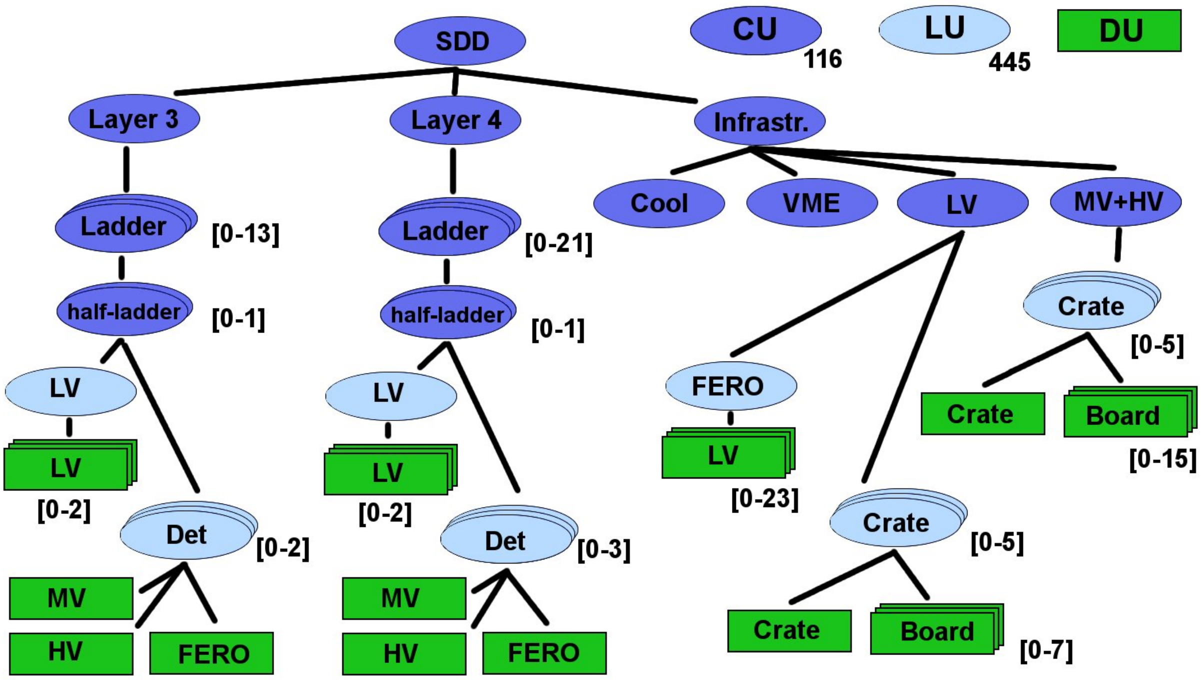

Figure 5.8: The finite state machine structure of the SDD [7].

Chapter 6

The PVSSII

In this chapter, I describe the main characteristics of the PVSSII program and I add a description of some of my applications written in the PVSSII.

6.1 Introduction

6.1.1 Overview

"PVSSII" [6, 12] is a German abbreviation of "Process visualization and control system II". It is a commercial software package designed for automation engineering, and is a core software for the control system. PVSSII was originally developed by an Austrian company 'ETM', but has been recently bought by Siemens.

6.1.2 PVSSII tools

The PVSSII is used to connect to the software devices, acquire the data they produce, and use them for their supervision, i.e. to monitor their behavior and to initialize, configure and operate them. To do that, the PVSSII provides the following components and tools:

Run-time database The place where the data from the devices are stored, and can be used for controlling, visualization, etc. purposes.

Archiving The data from the run-time database can be archived for the long term use.

Alarm generation and handling Alarms can be produced according to the data incoming from the devices. Those alarms are archived in the alarm database and can be handled specifically, depending on their content.

Graphical editor Allowing developers to make their own graphical user interface (panels).

Scripting language Allowing developers to interact with the data both, using the user interface or by background scripts that can work automatically. The PVSSII scripts follow the C++ syntax and include many SCADA-specific functions.

Graphical parametrization tool Allowing developers to define the structure of the databases (databases editor 'PARA') and application-specific alarms.

Drivers Providing the connection between PVSSII and the hardware or software to be supervised.

PVSSII applications are managed as 'projects' and contain all the information about their databases, panels, etc. All PVSSII projects are essentially made of the panels and the scripts. The panels are build using the graphical editor 'GEDI', included in the PVSSII.

6.1.3 Architecture

PVSSII has a highly distributed architecture. Every PVSSII application is composed of several processes, so called managers (see figure 6.1). These managers communicate via PVSSII-specific protocol over TCP/IP. The heart of the system is the Event Manager (EV), which is the only manager allowed to change the data in the databases. Moreover, drivers can be set to send data, when a significant change occurs, only to the event manager. Therefore, in a stable system (when no changes happen), no data traffic is present. Every PVSSII application contains one event manager and one database manager, and any number of drivers, user interfaces, etc.

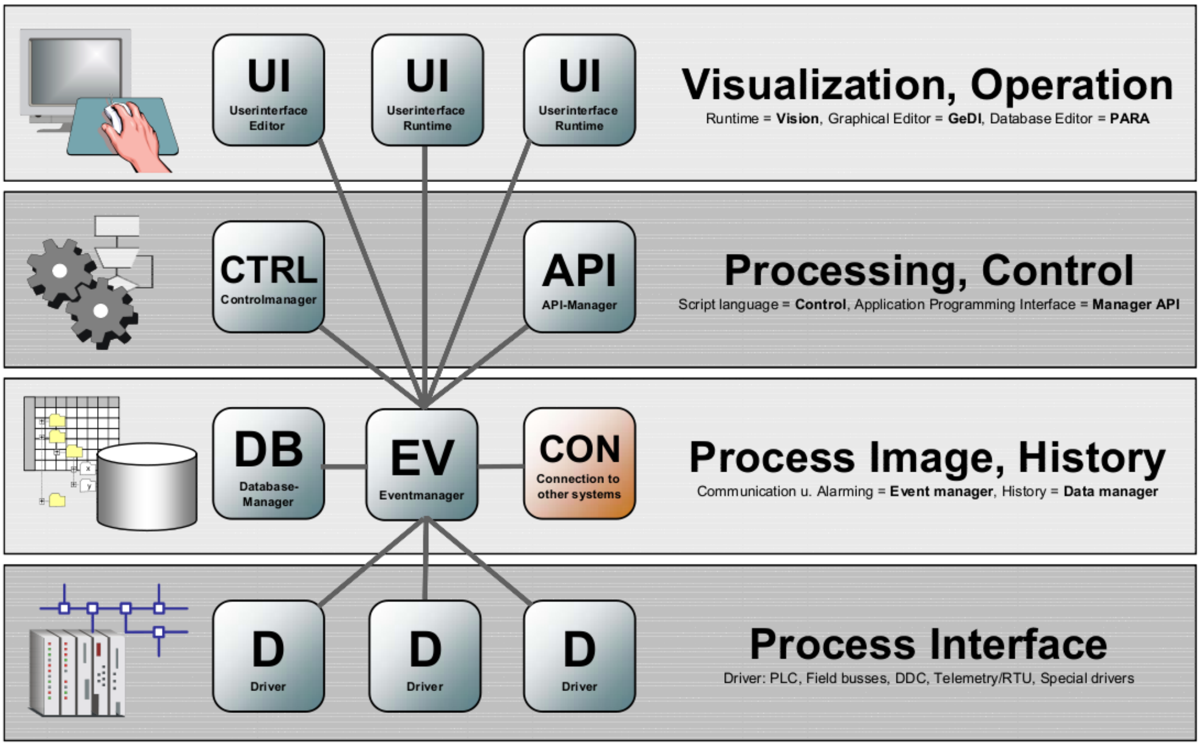

Figure 6.1: Managers in a typical PVSSII system [12].

The Event Manager (EV) is responsible for all the communication. It collects all the data from the devices and stores them in the run-time database. It also maintains the current data in memory. Moreover, it distributes the data to other managers.

The DataBase Manager (DB) provides the interacting with run-time database and archive.

User Interface Managers (UI) can get the device data from the database. They can also send data to the database, to be sent further to the devices.

Control Managers (Ctrl) provide background processes, by running the scripting language.

API Managers (API) allow developers to write their own programs that are able to access the databases, using the PVSSII-provided API.

Drivers (D) provide interface to the devices. Drivers can be PVSSII-provided or user-defined.

Archive Managers (not shown) allow users to archive data for later retrieval or viewing. An application may have one or more archive managers.

6.1.4 The Datapoint concept

PVSSII has its own run-time database, which allows storing data from the hardware devices. This database is designed in such a way that the data are easily accessible and can be treated as variables. Therefore, it has to be optimized for fast access. However, the stored data are difficult for accessing from outside the PVSSII. That is why the JCOP framework also includes an archiving tool.

The device data in the PVSSII run-time database are structured as, so called, 'DataPoints' (DP) of their predefined 'DataPoint Types' (DPT). The DPs/DPTs allow to model the devices by defining the DPs' structure. As such, the data associated with a particular device can be grouped together, instead of being held as separate variables. To interfere with the data in the DPs, PVSSII has a special editor called 'PARA'. It is also possible to interfere with them via scripts. In figure 6.2, the structure of one datapoint is shown in the PARA editor.

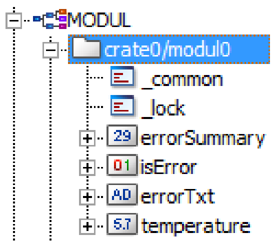

Figure 6.2: An example of the datapoint structure.

6.1.5 Distributed systems

The PVSSII managers can run both, on Microsoft Windows and Linux. Moreover, they can run in the same machine or can be distributed over different machines (including mixed Windows and Linux environments).

A distributed system is made by adding a 'Distribution Manager' (Dist), as shown in figure 6.3. Hundreds of systems can be connected this way. The figure also shows how an operator from a DCS panel can access a value on a sub-detector's device in such a distributed system.

6.2 SDD power supply simulation program in PVSSII

In this section, my PVSSII applications are described. These programs have been developed entirely for training purposes, but are, nevertheless, connected with the real DCS for ALICE silicon drift detectors. My task was to write a simulated power supply control system for ALICE SDDs.

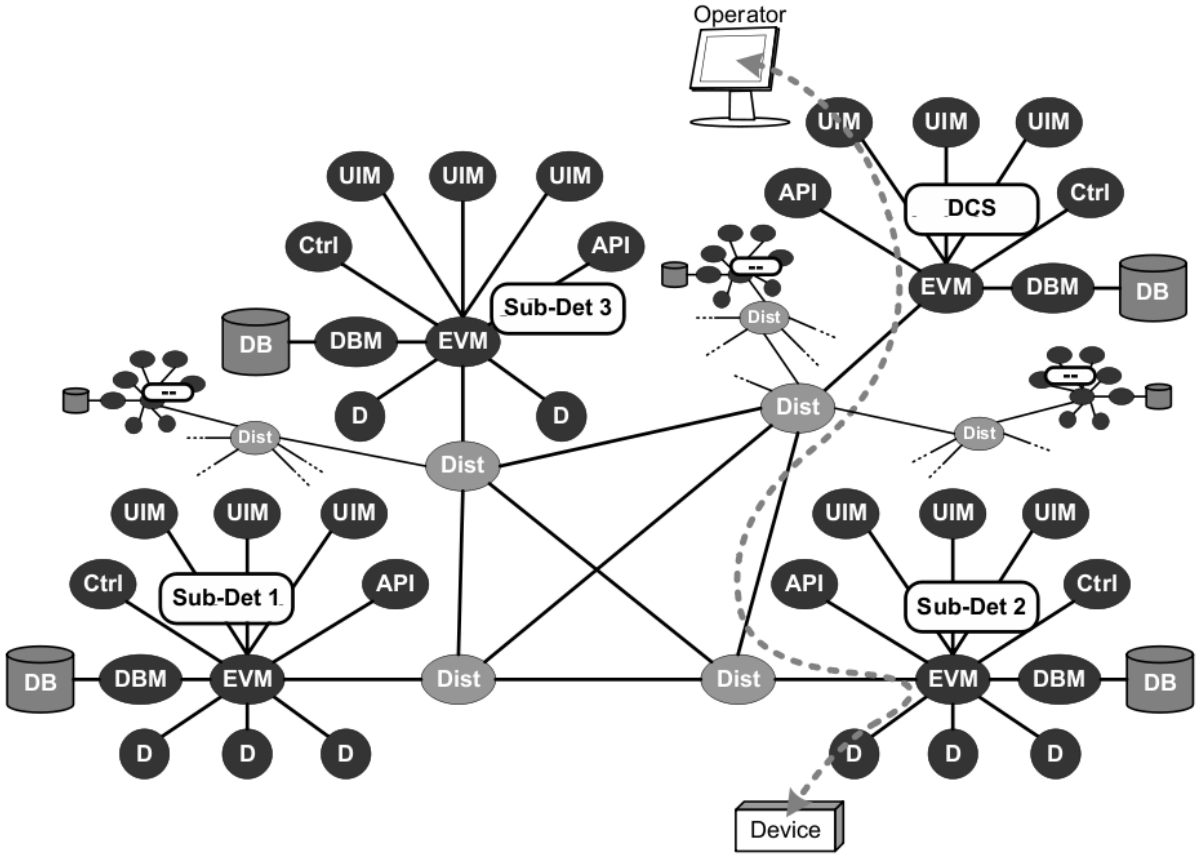

Figure 6.3: Distributed PVSSII system [6].

6.2.1 Datapoints and aliases

The power supply for the training applications is structured into four ‘crates’ (representing ladders in a SDD layer), each containing eight ‘modules’ of 16 ‘channels’ (8 medium-voltage and 8 high-voltage). The crates, their modules and channels can be turned on and off. The modules may be faulty, therefore they contain information, whether there has been an error and what error it is. They also measure their temperature. The channels can be put on and off, and also their voltage and current can be set.

The informations about the power supply devices have to be stored in PVSSII run-time database via datapoints, whose names are: “`crate0` – `3`” for crates, “`crateX\modul0` – `7`” for modules and “`crateX\modulY\channel00` – `15`” for channels, where `X` and `Y` are the parent crate’s and module’s numbers, respectively. Note that every module and every channel contains information of the crate and the module it belongs to. PVSSII allows the crates with all modules and channels to be included in one large DP. Processes with that DP, however, would work very slowly because of its size.

The downside of these DP names is that the chanels DPs’ names are very long. That is why PVSSII supports the datapoints’ aliases. Aliases to the channels DPs were given: “`MV1` – `256`” (as if for medium-voltage supply) to the channels with even numbers and “`HV1` – `256`” (for high-voltage) to the channels with odd numbers.

The datapoints’ structure is shown in figure 6.4. Every crate DP contains a boolean value that is set to ‘true’, if this crate is on. The module DPs are composed of a float value, representing its temperature, a boolean value that indicates, whether an error occurred, an integer value saying, what kind of error happened, and a string that contains the error message. Finally, the channel DPs consist of a boolean value indicating if this channel is on, two floats representing the set

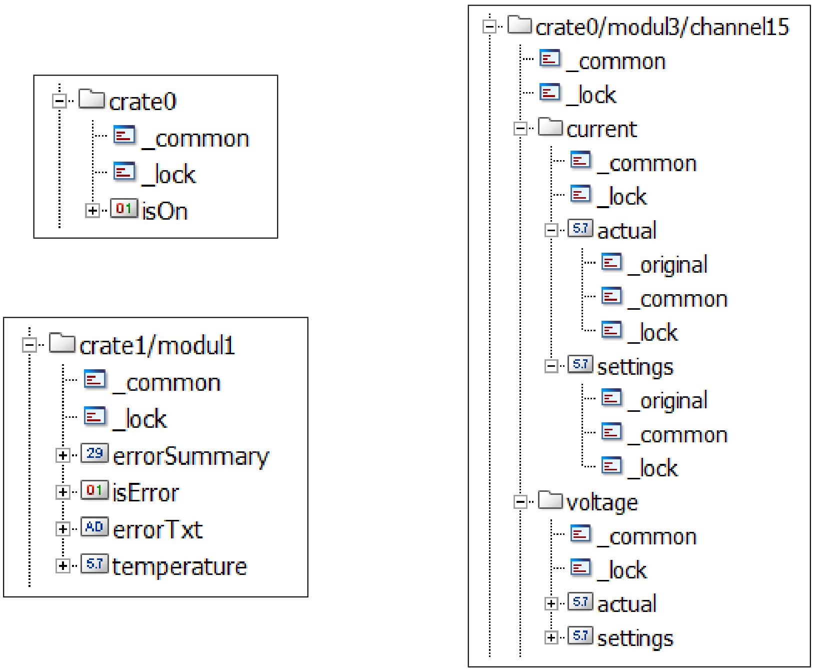

Figure 6.4: Structure of the datapoints that store data of the simulated power supply devices, as shown in the PARA editor.

and the actual measured value of voltage, and the same for the current.

The DPs can be managed via the PARA editor. This, however, is not very efficient (or possible) for their large number. Moreover, the user (operator) of the system does not have access to the PARA. Thus, a graphical user interface interface (GUI) had to be implemented. In figure 6.5, the GUI for managing the datapoints is shown, there are: a button that creates the DPs, one that deletes them and one that gives them the aliases. The window also includes a text-box for communicating with the user.

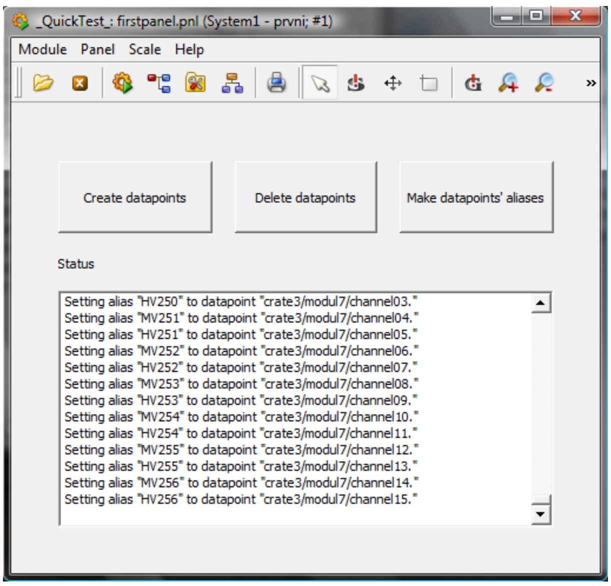

Figure 6.5: Window for managing the datapoints.

6.2.2 Supervising of the power supply (panels)

The next task was to create a graphical user interface for the supervision of the power supply. PVSSII provides a very helpful feature, called 'panel referencing'. This feature allows to add a panel with specific data, like the channel's number, to a window (in PVSSII called a 'module').

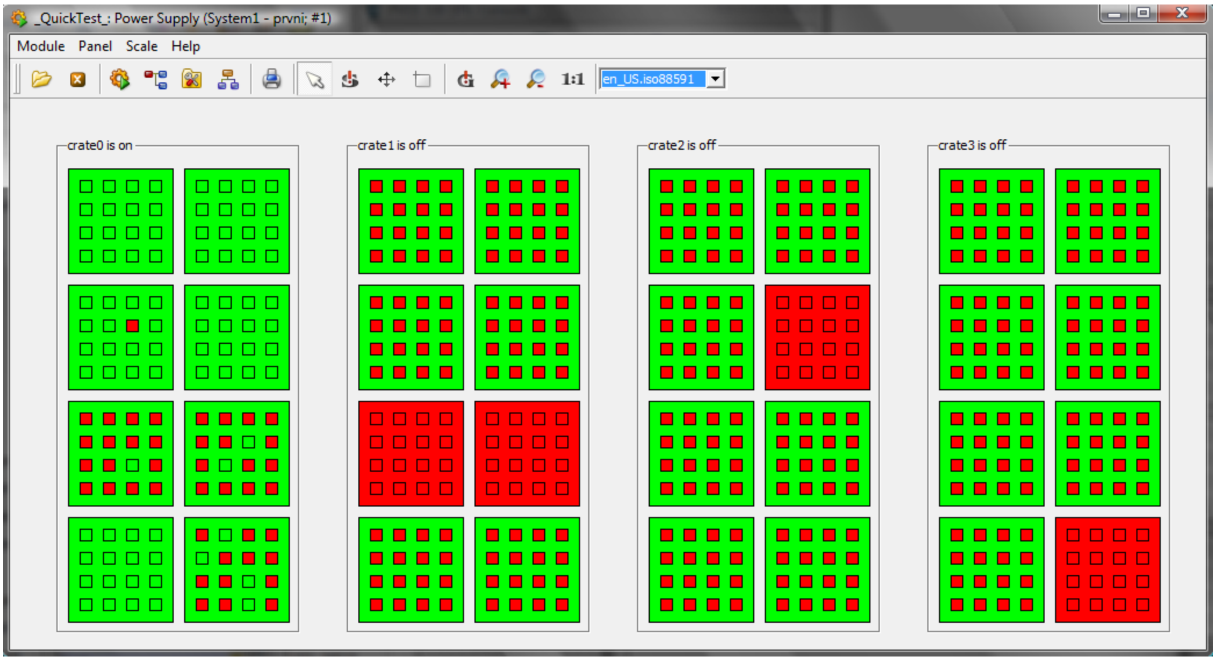

Figure 6.6: Window for the supervision of the whole power supply.

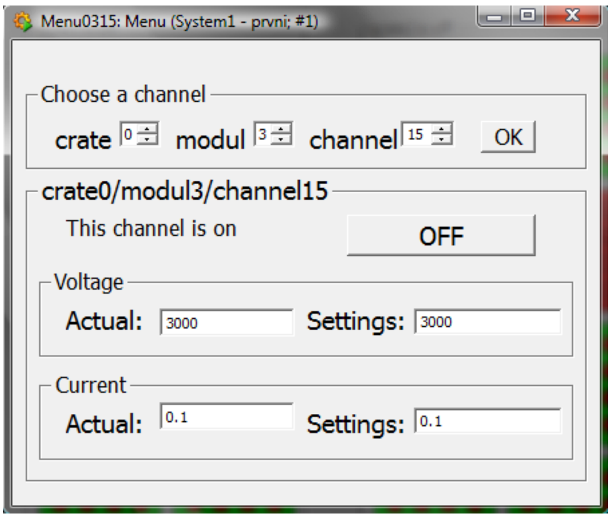

Figure 6.7: Window for controlling the channels.

For the window for the supervision of the whole power supply (figure 6.6), four 'crate panels' with numbers 0 – 3 were added. Each crate panel contains eight 'module panels' with 16 'channel panels' each. To each panel, the proper numbers of its position were addressed.

The simplest, channel panel, contains only one little square that indicates, whether the channel is on (green color) or off (red color). It also activates a pop-up window for controlling its channel, when clicked. The module panel is a slightly larger square that turns red when its module has an error (otherwise it is green). It also includes its 16 channel panels. The largest one, crate panel, contains a frame with its number and information whether it is on or off, and its 8 module panels.

The control window for channels is shown in figure 6.7. It contains text-boxes with its voltage and current values, and also an on/off button. There is also a switch between the channels. The control windows for modules and channels are very similar.

6.2.3 Simulated run of the power supply (background scripts)

To learn how to write scripts that run in the background of the PVSSII, my next task was to write a very simple simulator of the run of the power supply. The aim was more at learning with the scripting language than at simulating the reality.

The first script simply checks the database every five seconds and assigns the value from the 'set' voltage and current to the 'actual' voltage and current. The second script connects the on/off value on the crate DPs with the current and voltage values of their channels. When a crate is turned 'on', all its channels are turned on and its HV channels are set to 3000V and 0.1A, and its LV channels are set to 40V and 0.05A. When a crate is turned off, all its channels are also turned off and all their values are set to zero.

Chapter 7

Conclusion

ALICE detector has the largest number of sub-detectors of all the four LHC experiments. Therefore, the DCS for ALICE is a very complex system with very strict requirements which can be fulfilled, though, by using normalized solutions.

The commercial SCADA, PVSSII, was chosen as a core software for the DCS for its many benefits that make developing of the control software easier. It also provides many solutions to the ALICE DCS requirements. However, some specific features have to be added via the JCOP and ALICE frameworks. As the PVSSII has been bought by the Siemens company only recently, it is unclear whether some changes will occur or not.

In the PVSSII programs, I have learned how to use the main features of the PVSS, such as datapoints, panels and background scripts, as well as the standard principles of programming of the control systems. These programs were made with a standard graphical user interface that ensure an easy and intuitive operation of the DCS.

In the future, I would like to contribute to the development of the ALICE SDD's control system because it will experience vast changes because of the planned unification of all the ITS detector control systems.

List of Figures

List of Abbreviations

ACORDE .... ALICE Cosmic Ray Detector

ACR .... ALICE Control Room

ALICE .... A Large Ion Collider Experiment

AMBRA .... SDD Digital event buffer

APD .... Avalanche Photo-Diode

ASIC .... Application-Specific Integrated Circuit

CARLOS .... SDD Zero suppressor

CERN .... Centre Européenne pour Recherche Nucléaire (European Organization for Nuclear Research)

CPV .... Charged-Particle Veto detector

CTP .... Central Trigger Processor

CU .... Control Unit

DAQ .... Data Acquisition

DCS .... Detector Control System

DCU .... Detector Control Unit

DDL .... Detector Data Link

DIM .... Distributed Information Management

DIP .... Data Interchange Protocol

DP .... DataPoint

DPT .... DataPoint Type

DU .... Device Unit

ECS .... Experiment Control System

EMCal .... ElectroMagnetic CALorimeter

FERO .... Front-end electronics and readout

FMD .... Forward Multiplicity Detector

FPGA .... Field-Programmable Gate Array

FSM .... Finite State Machine

GOL .... Gigabit Optical Link

HLT .... High-Level Trigger

HMPID .... High Momentum Particle Identification Detector

IP .... Interaction Point

ITS .... Inner Tracking System

JTAG .... Joined Test Action Group

L0 .... Level-0 trigger

L1 .... Level-1 trigger

L2 .... Level-2 trigger

LEP .... Large Electron-Positron Collider

LHC .... Large Hadron Collider

LU .... Logical Unit

MCM .... Multi-Chip Module

MOS .... Metal-Oxide Semiconductor

MRPC .... Multi-Gap Resistive-Plate Chamber

PASCAL .... SDD Multi purpose ASICs

PHOS .... Photon Spectrometer

PID .... Particle IDentification

PLC .... Programmable Logic Controller

PMD .... Photon Multiplicity Detector

PVSS .... Prozessvisualierungs- und Steuerungs-System (Process Visualization and Control System)

QCD .... Quantum ChromoDynamics

QGP .... Quark-Gluon Plasma

RHIC .... Relativistic Heavy Ion Collider

RICH .... Ring Imaging Cherenkov detector

SCADA .... Supervisory Controls and Data Acquisition

SDD .... Silicon Drift Detector

SPD .... Silicon Pixel Detector

SSD .... Silicon Strip Detector

T0 .... Time 0 detector

TOF .... Time-of-Flight

TPC .... Time-Projection Chamber

TRD .... Transition Radiation Detector

TRG .... Trigger system

V0 .... Vertex 0 detector

VME .... Versa Module Eurocard

ZDC .... Zero Degree Calorimeter

ZEM .... ZDC ElectroMagnetic calorimeter

Bibliography

[1] ALICE Collaboration, *The ALICE experiment at the CERN LHC*, *JINST* 3 S08002 (2008).

[2] ALICE collaboration, *Technical proposal for A Large Ion Collider Experiment at the CERN LHC*, CERN-LHCC-95-71, http://cdsweb.cern.ch/record/293391.

[3] F. Carminati et al., *ALICE: physics performance report, volume I*, J. Phys. G 30 (2004) 1517.

[4] B. Alessandro et al., *ALICE: physics performance report, volume II*, J. Phys. G 32 (2006) 1295.

[5] ALICE collaboration, *ALICE Inner Tracking System (ITS): Technical Design Report*, CERN-LHCC-99-012, http://edms.cern.ch/file/398932/1.

[6] ALICE collaboration, *ALICE trigger data-acquisition high-level trigger and control system: Technical Design Report*, CERN-LHCC-2003-062, http://cdsweb.cern.ch/record/684651.

[7] *Official web pages of the ALICE DCS*, http://alicedcs.web.cern.ch/alicedcs/.

[8] J. Král, *Research project (Výzkumný úkol)*, Czech Technical University in Prague, Faculty of Nuclear Sciences and Physical Engineering, Prague (2007).

[9] *JCOP*, http://itco.web.cern.ch/itco/Projects-Services/JCOP/welcome.html.

[10] P.C. Burkimsher, *JCOP experience with a commercial SCADA product PVSS, Proceedings of the ICALEPCS 2003*, Gyeongju Korea (2003), http://cdsweb.cern.ch/record/924942.

[11] A. Daneels and W. Salter, *Selection and evaluation of commercial SCADA systems for the controls of the Cern LHC experiments, Proceedings of the ICALEPCS99 conference*, Trieste Italy (1999), http://cdsweb.cern.ch/record/532627.

[12] B. Briss, M. Schagginger, L. Knipp, *PVSS II getting started*, (2004), http://j2eeps.cern.ch/wikis/download/attachments/14778428/0407PVSS_II_GettingStarted_Basics_en.pdf?version=1&modificationDate=1299054760000.

[13] D. Brand and P. Zafiropulo, *On Communicating Finite-State Machines*, Journal of the Association for Computing Machmery Vol 30 No 2 (1983) 323.

[14] A. Daneels and W. Salter, *What is SCADA?, Proceedings of the ICALEPCS99 conference*, Trieste Italy (1999), https://accelconf.web.cern.ch/accelconf/ica99/papers/mc1i01.pdf.

[15] The OPC Foundation, *About OPC*, http://www.opcfoundation.org/Default.aspx/01_about/01_whatis.asp.

[16] A. Morsch and B. Pastircak, *Radiation in ALICE detectors and electronic racks*, ALICE Internal Note ALICE-INT-2004-017, http://edms.cern.ch/file/358706/1.

[17] *Code E - Fire protection*, EDMS Id: 335728, http://edms.cern.ch/file/335728/2.01/;

Code F Rev. Radiation Protection, EDMS Id: 335729, http://edms.cern.ch/file/335729/2/;

IS 5 Emergency stop, EDMS Id: 335742, http://edms.cern.ch/file/335742/2/;

IS 37 Alarms and alarm systems, EDMS Id: 335802, http://edms.cern.ch/file/335802/4/.

[18] J. Gerndt and P. Průša, *Detektory Ionizujícího záření*, Vydavadelství ČVUT, Prague (2011).

[19] E. Cerron-Zeballos et al., *A new type of resistive plate chamber: the multigap RPC*, Nucl. Instrum. Meth. A 374 (1996) 132.

[20] Y. Andres et al., *R&D in ALICE: the CsI-based RICH high momentum particle identification detector*, Eur. Phys. J. Direct. C 4 (2002) 25.

[21] R. Arnaldi et al., *Spatial resolution of RPC in streamer mode*, Nucl. Instrum. Meth. A 490 (2002) 51.

[22] F. Antinori et al., *Experience with a 30 cm^2 silicon pixel plane in CERN experiment WA97*, Nucl. Instrum. Meth. A 360 (1995) 91.

[23] C. Garabatos, *The ALICE TPC*, Nucl. Instrum. Meth. A 535 (2004) 197.

[24] D. Nouais et al., *The ALICE silicon drift detector system*, Nucl. Instrum. Meth. A 501 (2003) 119, ALICE-PUB-2001-59, http://cdsweb.cern.ch/record/531804.

[25] A. Rashevsky et al., *Characteristics of the ALICE Silicon Drift Detector*, Nucl. Instrum. Meth. A 461 (2001) 133.

[26] M. Sitta, *The Silicon Drift Detector of the ALICE experiment*, Nucl. Instrum. Meth. A 611 (2010) 591.